Weak decays of $\bar{B}_s$ mesons

C. Albertus
Departamento de Física Atómica, Molecular y Nuclear. Universidad de Granada.
Avenida de Fuentenueva S/N, E-18071 Granada, Spain

In the present work we study the semileptonic decays of $\bar{B}_s$ mesons in the context of nonrelativistic constituent quark models. We estimate the uncertainties of our calculation using different interquark potentials to obtain the meson wave functions. We check the results from our model against the predictions of Heavy Quark Symmetry, in the limit of infinite heavy quark mass. We also study the nonleptonic decays of $\bar{B}_s$ mesons within the factorization approximation.

arXiv:1401.1791v1 [hep-ph] 8 Jan 2014

I. INTRODUCTION

Since the first claims on the existence of B_s and $\bar{B_s}$, both their lifetimes, decay modes [1–12] and oscillations [13–19] have been objectives of the uttermost interest of experimental collaborations. Being below the $B-K$ threshold, it can only decay by means of mechanisms governed by electroweak currents, making it an ideal system to study the physics of the weak interaction in the presence of heavy quarks.

A considerable amount of the work devoted to the b-meson sector involve the ideas of Heavy Quark Symmetry [20, 21] (HQS). HQS is an approximate symmetry of QCD that becomes exact in the limit in which the mass of the heavy quark becomes infinity. This symmetry establishes that in such a limit, the quantum numbers of the light degrees of freedom are all well defined, and independent of the heavy quark flavor and spin. This is similar, for instance, to what happens in atomic physics, where electron properties are approximately independent of the mass and spin of the nucleus for a fixed nuclear charge. Heavy Quark Symmetry can be cast into the language of an effective theory, leading to Heavy Quark Effective Theory [22] (HQET). HQET enables a systematic, order by order evaluation of the corrections to the infinity mass limit in the inverse powers of the heavy quark masses. Besides, HQET allows theoretical control of the non-perturbative aspects of the calculation in the proximities of the infinite quark mass limit. At leading order in an expansion on the heavy quark mass only one form factor, the Isgur-Wise function remains, largely simplifying the description of the decay. However, HQS does not determine the Isgur-Wise function: one still needs to implement some other nonperturbative method.

HQS leads to many more model independent predictions. The most remarkable of those for the meson sector, is the fact that the masses of pseudoscalar and vector mesons are degenerate in the heavy quark limit. Nonrelativistic quark models fulfil this constrain: the reduced mass of the two quarks is just the mass of the light one, and the spin-spin terms, which can distinguish vector from pseudoscalar, are suppressed by the mass of the heavy quark, becoming exactly zero in the HQS limit. At this point, one important question is to what extent do the deviations from the HQS limit, evaluated from nonrelativistic quark models agree with the constraints predicted by HQET. Furthermore, it is possible to make use of the HQET constrains to improve the predictions of the quark models. In the previous work of Ref. [23], we studied the leptonic and semileptonic decays of B mesons, and considered the implications of HQS. The nonleptonic and semileptonic decay of B_c mesons (where presence of two heavy quarks leads to infrared divergences that break the flavor symmetry, and subsequently only Heavy Quark Spin Symmetry remains), has been considered in Ref. [24]. In Refs. [25–27] we calculated the semileptonic decay widths of baryons containing one or two heavy quarks, and worked out the symmetry implications on the observables.

Some of the decay modes of B_s or $\bar{B_s}$ mesons have been studied within the framework of relativistic constituent quark model [28, 29], perturbative QCD [30, 31], Bethe-Salpeter techniques [32], light front quark model [33], sum rules [34–36] or non relativistic constituent quark model [37] for instance. In this paper we study the semileptonic and nonleptonic decay of $\bar{B_s}$ in the context of nonrelativistic constituent quark model. The rest of the paper is organized as follows. In Section II we describe the meson states for the different values of J^P and the quark models used in this work. In Sec. III we give the form factor decomposition of the weak decay matrix elements and calculate the decay width, both for light (e,μ) and heavy (τ) charged lepton. We also work in the helicity formalism [38]. Besides, we study the implications of HQS in these decays. In Sec. V the problem of nonleptonic two meson decays of B_s is studied. The meson decay constants required in Sec. V and the CKM matrix elements used both in Secs. III and V can be found in Tables II, respectively, while the different D_s states considered in the semileptonic and some nonleptonic decays studied in this paper and their quantum numbers are summarized in Table I. For the $D_s^1(2460)$ and $D_s^1(2536)$ states, we assume that they are mixing of $^3P_1$ and $^1P_1$ $c\bar{s}$ states, with a mixing angle of 34.5°, as in Ref. [28]. In Sec. VII we present a summary and our conclusions. The paper also includes an Appendix to clarify some technical details of our work.

	Mass (MeV)
$\bar{B_s}(0^-)$	5366.77 [39]
$D_s^+(0^-)$	1968.49 [39]
$D_{s0}^{*+}(2317)(0^+)$	2317.8 [39]
$D_s^{*+}(1^-)$	2112.3 [39]
$D_{s1}(2460)$	2459.6 [39]
$D_{s1}(2536)$	2535.12 [39]
$c\bar{s}(2^-)$	2806.9
$D_{s2}(2573)^+(2^+)$	2571.9 [39]

TABLE I. Masses of the states involved in this calculation.

II. MESON STATES AND INTERQUARK INTERACTIONS

In the context of nonrelativistic constituent quark models, the state of a meson M is written as [40]:

$$\begin{aligned}\left|M;\lambda\vec{P}\right\rangle_{\rm NR} &= \int d^3p \sum_{\alpha_1\alpha_2} \hat{\phi}^{(M,\lambda)}_{\alpha_1\alpha_2}(\vec{p}) \frac{(-1)^{(1/2)-s_2}}{(2\pi)^{3/2}\sqrt{(2E_{f_1}(\vec{p}_1))(2E_{f_2}(\vec{p}_2))}} \\ &\times \left|q,\alpha_1\,\vec{p}_1 = \frac{m_{f_1}}{m_{f_1}+m_{f_2}}\vec{P}-\vec{p}\right\rangle \left|\bar{q},\alpha_2\,\vec{p}_2 = \frac{m_{f_2}}{m_{f_1}+m_{f_2}}\vec{P}+\vec{p}\right\rangle,\end{aligned} \tag{1}$$

where $\vec{P}$ is the meson three momentum, while λ labels the spin projection in the meson center of mass. The index α_i represent the quantum numbers of spin, flavor and color of the quark and the antiquark, with four momentum and mass given by $(E_{f_i}(\vec{p}_i),\vec{p}_i)$ and m_{f_i} respectively. The factor $(-1)^{1/2-s_2}$ ensures that the antiquark spin states have the correct phase [1].

The normalization of quark and antiquark states is

$$\left\langle \alpha'\vec{p}\,'|\alpha\vec{p}\right\rangle = 2E_f\delta_{\alpha'\alpha}\delta^3(\vec{p}-\vec{p}\,')(2\pi)^3 \tag{2}$$

As for the momentum wave function accounting for the relative motion of the quark-antiquark system, the normalization is given by

$$\int d^3p \sum_{\alpha_1\alpha_2} (\hat{\phi}^{M,\lambda'}_{\alpha_1\alpha_2}(\vec{p}))^* \hat{\phi}^{M,\lambda}_{\alpha_1\alpha_2}(\vec{p}) = \delta_{\lambda\lambda'}, \tag{3}$$

and finally, the normalization of the meson states in our model is

$${}_{\rm NR}\left\langle M\lambda'\vec{P}'|M\lambda\vec{P}\right\rangle_{\rm NR} = \delta_{\lambda\lambda'}(2\pi)^3\delta(\vec{P}'-\vec{P}). \tag{4}$$

In this calculation we will need the ground state wave function for scalar (0^+), pseudoscalar (0^-), vector (1^-), axial-vector (1^+), tensor (2^+) and pseudotensor (2^-). Assuming always a value for the orbital angular momentum as low as possible, we have for a meson M with scalar, pseudoscalar and vector quantum numbers

$$\begin{aligned}\hat{\phi}^{(M(0^+))}_{\alpha_1,\alpha_2}(\vec{p}) &= \frac{1}{\sqrt{3}}\delta_{c_1c_2}\hat{\phi}^{(M(0^+))}_{(s_1,f_1),(s_2,f_2)}(\vec{p}) = \frac{i}{\sqrt{3}}\delta_{c_1c_2}\hat{\phi}^{(M(0^+))}_{f_1,f_2}(|\vec{p}\,|)\sum_m (1/2,1/2,1;s_1,s_2,-m)(1,1,0;m,-m,0)Y_{1m}(\hat{p}) \\ \hat{\phi}^{(M(0^-))}_{\alpha_1,\alpha_2}(\vec{p}) &= \frac{1}{\sqrt{3}}\delta_{c_1c_2}\hat{\phi}^{(M(0^-))}_{(s_1,f_1),(s_2,f_2)}(\vec{p}) = \frac{-i}{\sqrt{3}}\delta_{c_1c_2}\hat{\phi}^{(M(0^-))}_{f_1,f_2}(|\vec{p}\,|)(1/2,1/2,0;s_1,s_2,0)Y_{00}(\hat{p}) \\ \hat{\phi}^{(M(1^-),\lambda)}_{\alpha_1,\alpha_2}(\vec{p}) &= \frac{1}{\sqrt{3}}\delta_{c_1c_2}\hat{\phi}^{(M(1^-),\lambda)}_{(s_1,f_1),(s_2,f_2)}(\vec{p}) = \frac{-1}{\sqrt{3}}\delta_{c_1c_2}\hat{\phi}^{(M(1^-))}_{f_1,f_2}(|\vec{p}\,|)(1/2,1/2,1;s_1,s_2,0)Y_{00}(\hat{p}),\end{aligned} \tag{5}$$

where $(j_1,j_2,j_3,m_1,m_2,m_3)$ are Clebsch-Gordan coefficients, Y_{lm} are spherical harmonics and $\hat{\phi}_{f_1,f_2}(|\vec{p}\,|)$ is the Fourier transform of the radial, coordinate space, wave function.

Axial vector mesons require orbital angular momentum $L=1$, and in this case the two possible values of the total quark-antiquark spin $S_{q\bar{q}}=0,1$ are allowed. Thus, there are two possible states:

$$\begin{aligned}\hat{\phi}^{(M(1^+),S_{q\bar{q}}=0,\lambda)}_{\alpha_1,\alpha_2}(\vec{p}) &= \frac{1}{\sqrt{3}}\delta_{c_1c_2}\hat{\phi}^{(M(1^+),S_{q\bar{q}}=0,\lambda)}_{(s_1,f_1),(s_2,f_2)}(\vec{p}) = \frac{-1}{\sqrt{3}}\delta_{c_1c_2}\hat{\phi}^{(M(1^+),S_{q\bar{q}}=0)}_{f_1,f_2}(|\vec{p}\,|)(1/2,1/2,0;s_1,s_2,0)Y_{1\lambda}(\hat{p}) \\ \hat{\phi}^{(M(1^+),S_{q\bar{q}}=1,\lambda)}_{\alpha_1,\alpha_2}(\vec{p}) &= \frac{1}{\sqrt{3}}\delta_{c_1c_2}\hat{\phi}^{(M(1^+),S_{q\bar{q}}=1,\lambda)}_{(s_1,f_1),(s_2,f_2)}(\vec{p}) \\ &= \frac{-1}{\sqrt{3}}\delta_{c_1c_2}\hat{\phi}^{(M(1^+),S_{q\bar{q}}=1)}_{f_1,f_2}(|\vec{p}\,|)\sum_m (1/2,1/2,1;s_1,s_2,\lambda-m)(1,1,1;m,\lambda-m,\lambda)Y_{1m}(\hat{p}).\end{aligned} \tag{6}$$

f_π	f_ρ	f_K	f_{K^*}	f_D	$f_{D^*}\dagger$	f_{D_s}	$f_{D_s^*}\dagger$	$f_\Phi\dagger$	$f_{J/\Psi}\dagger$	$\lvert V_{cb}\rvert$	$\lvert V_{ud}\rvert$	$\lvert V_{us}\rvert$	$\lvert V_{cs}\rvert$	$\lvert V_{cd}\rvert$
130.41	210	159.8	217	206.7	222	260	318	312.6	488.5	0.0413	0.9743	0.2240	0.9734	0.2252

TABLE II. Values for the meson decay constants in MeV and Cabibbo-Kobayashi-Maskawa matrix elements used through this work. The decay constants marked with a † have been calculated using our model.

[1] Under charge conjugation C, quark and antiquark states are related via $\mathcal{C}c^\dagger_\alpha\mathcal{C}^\dagger = (-1)^{1/2-s}d^\dagger_\alpha(\vec{p})$, so the antiquark states with the correct spin relative phase are $(-1)^{1/2-s}d^\dagger_\alpha(\vec{p})|0\rangle = (-1)^{1/2-s}|\bar{q},\alpha\vec{p}\rangle$

For tensor and pseudotensor mesons, the wave functions can be written as:

$$\begin{aligned}
\hat{\phi}^{(M(D_{s2}^*),\lambda)}_{\alpha_1,\alpha_2}(\vec{p}) &= \frac{1}{\sqrt{3}}\delta_{c_1c_2}\hat{\phi}^{(M(D_{s2}^*),\lambda)}_{(s_1,f_1),(s_2,f_2)}(\vec{p}) \\
&= \frac{1}{\sqrt{3}}\delta_{c_1c_2}\hat{\phi}^{(M(D_{s2}^*))}_{f_1,f_2}(|\vec{p}|)\sum_m(1/2,1/2,1;s_1,s_2,\lambda-m)(1,1,2;m,\lambda-m,\lambda)Y_{1m}(\hat{p}) \\
\hat{\phi}^{(M(2^-),\lambda)}_{\alpha_1,\alpha_2}(\vec{p}) &= \frac{1}{\sqrt{3}}\delta_{c_1c_2}\hat{\phi}^{(M(2^-),\lambda)}_{(s_1,f_1),(s_2,f_2)}(\vec{p}) \\
&= \frac{-1}{\sqrt{3}}\delta_{c_1c_2}\hat{\phi}^{(M(2^-))}_{f_1,f_2}(|\vec{p}|)\sum_m(1/2,1/2,1;s_1,s_2,\lambda-m)(2,1,2;m,\lambda-m,\lambda)Y_{2m}(\hat{p})
\end{aligned} \tag{7}$$

In the previous expressions, all phases have been introduced for later convenience.

We consider five different interquark potentials to calculate the coordinate space wave functions, one proposed by Bhadury [41] and other four proposed by Silvestre-Brac in [42]. All of them have the same structure: a term accounting for confinement, plus Coulomb and hyperfine terms both of them coming from one-gluon exchange. They differ from one another in the form factors present in the hyperfine term, the power of the confinement term, or the presence of a form factor in the Coulomb one-gluon exchange term. All free parameters have been adjusted to reproduce light and heavy-light meson spectra. We have successfully used these potentials before to describe the spectra and decays of charmed and bottom baryons.

The different results obtained with the different potentials provide us with an estimation of the theoretical error. It has to be mentioned that another source of theoretical uncertainty that we cannot account for is the use of nonrelativistic kinematics in the evaluation of the wave function. While this approximation is not, a priori, a good choice in the presence of light quarks, one has to notice that all nonrelativistic potentials have free parameters fitted to experimental data. Hence, one can argue that the ignored relativistic effects are partially included in the fitted values of the parameters.

III. SEMILEPTONIC DECAYS

In this section we will consider the semileptonic decay of $\bar{B_s}$ mesons into different D_s meson states with 0^+, 0^-, 1^+, 1^-, 2^+ and 2^- spin-parity quantum numbers. These decays correspond to $b\to c$ transition at the quark level governed by the current

$$J^{cb}_\mu(0) = J^{cb}_{V\mu}(0) - J^{cb}_{A\mu}(0) = \bar{\Psi}_c(0)\gamma_\mu(I-\gamma_5)\Psi_b(0), \tag{8}$$

with Ψ_f a quark field with flavor f.

A. Form factor decomposition of hadronic matrix elements

The hadronic matrix elements involved in these processes can be parametrized in terms of form factors as:

$$\begin{aligned}
\left\langle D_s^+,\vec{P}_{D_s}\left|J^{bc}_\mu(0)\right|\bar{B_s},\vec{P}_{\bar{B_s}}\right\rangle &= P_\mu F_+(q^2) + q_\mu F_-(q^2) \\
\left\langle D_s^{*+},\lambda\vec{P}_{D_s^*}\left|J^{bc}_\mu(0)\right|\bar{B_s},\vec{P}_{\bar{B_s}}\right\rangle &= \frac{-1}{m_{\bar{B_s}}+m_{D_s^*}}\varepsilon_{\mu\nu\alpha\beta}\varepsilon^{\nu *}_{(\lambda)}(\vec{P}_{c\bar{s}})P^\alpha q^\beta V(q^2) \\
&\quad - i\left\{(m_{\bar{B_s}}-m_{D_s^*})\varepsilon^*_{(\lambda)\mu}(\vec{P}_{c\bar{s}})A_0(q^2) - \frac{P\cdot\varepsilon^*_{(\lambda)}(\vec{P}_{D_s^*})}{m_{\bar{B_s}}+m_{D_s^*}}(P_\mu A_+(q^2)+q_\mu A_-(q^2))\right\} \\
\left\langle D_{s2}^{*+},\lambda\vec{P}_{D_{s2}^*}\left|J^{bc}_\mu(0)\right|\bar{B_s},\vec{P}_{\bar{B_s}}\right\rangle &= \varepsilon_{\mu\nu\alpha\beta}\varepsilon^{\nu\delta *}_{(\lambda)}(\vec{P}_{D_{s2}^*})P_\delta P^\alpha q^\beta T_4(q^2) \\
&\quad - i\left\{\varepsilon^*_{(\lambda)\mu\delta}(\vec{P}_{D_{s2}^*})P^\delta T_1(q^2) + P^\nu P^\delta \varepsilon^*_{(\lambda)\nu\delta}(\vec{P}_{D_{s2}^*})(P_\mu T_2(q^2)+q_\mu T_3(q^2))\right\},
\end{aligned} \tag{9}$$

where $P_{\bar{B_s}}$ and $P_{c\bar{s}}$ (with $c\bar{s}=D_s,D_s^*,D_{s2}^*$) are the meson four-momenta, $m_{\bar{B_s}}$ and $m_{c\bar{s}}$ their masses respectively, $P=P_{\bar{B_s}}+P_{c\bar{s}}$, $q=P_{\bar{B_s}}-P_{c\bar{s}}$. $\varepsilon^{\mu\nu\alpha\beta}$ is the fully antisymmetric tensor, for which we have taken the convention $\varepsilon^{0123}=1$. q^2 ranges from $q^2_{\min}=m_l^2$ to $q^2_{\max}=(P_{\bar{B_s}}-P_{c\bar{s}})^2$. It is common to use $\omega=(m^2_{\bar{B_s}}-m^2_{c\bar{s}}-q^2)/2m_{\bar{B_s}}m_{c\bar{s}}$ instead of q^2, corresponding $\omega_{\min}=1$ to

$q^2_{\rm max}$. $\varepsilon_{(\lambda)\mu}(\vec{P})$ and $\varepsilon_{(\lambda)\mu\nu}(\vec{P})$ are the polarization vector and tensor of vector and tensor mesons, respectively. The latter can be evaluated as

$$\varepsilon^{\mu\nu}_{(\lambda)}(\vec{P}) = \sum_m (1,1,2;m,\lambda-m,\lambda)\varepsilon^{\mu}_{(\lambda)}(\vec{P})\varepsilon^{\nu}_{(\lambda-m)}(\vec{P}). \tag{10}$$

The different polarization vectors used in this work can be found in the Appendix of Ref. [40].

Meson states in Eq. (9) are normalized as

$$\left\langle M,\lambda'\vec{P}'|M\lambda\vec{P}\right\rangle = \delta_{\lambda'\lambda}2E_M(\vec{P})(2\pi)^3\delta(\vec{P}-\vec{P}'), \tag{11}$$

where $E_M(\vec{P})$ is the energy of the meson M with three momentum $\vec{P}$. The factor $2E_M$ should be noticed, in contrast with Eq. (4).

For 0^+, 1^+ and 2^- final states the form factor decomposition is the same as for the 0^-, 1^- and 2^+ cases above, where just $-J^{cb}_A(0)$ is contributing instead of $J^{cb}_V(0)$ and vice versa.

B. Decays into scalar and pseudoscalar states

In this section we will consider the decay of $\bar{B_s}$ mesons into pseudoscalar and scalar $c\bar{s}$ mesons. For $\bar{B_s}\to D_s^+$, i. e. (0^-) transitions, the form factors are given by

$$\begin{aligned}
F_+(q^2) &= \frac{1}{m_{\bar{B_s}}}\left(V^0(|\vec{q}|) + \frac{V^3(|\vec{q}|)}{|\vec{q}|}(E_{D_s}(-\vec{q}) - m_{D_s})\right)\\
F_-(q^2) &= \frac{1}{m_{\bar{B_s}}}\left(V^0(|\vec{q}|) + \frac{V^3(|\vec{q}|)}{|\vec{q}|}(E_{D_s}(-\vec{q}) + m_{D_s})\right)
\end{aligned} \tag{12}$$

whereas for a transition onto a $D^{*+}_{s0}(0^+)$ state we have

$$\begin{aligned}
F_+(q^2) &= \frac{-1}{m_{\bar{B_s}}}\left(V^0(|\vec{q}|) + \frac{V^3(|\vec{q}|)}{|\vec{q}|}(E_{D^*_{s0}}(-\vec{q}) - m_{D^*_{s0}})\right)\\
F_-(q^2) &= \frac{-1}{m_{\bar{B_s}}}\left(V^0(|\vec{q}|) + \frac{V^3(|\vec{q}|)}{|\vec{q}|}(E_{D^*_{s0}}(-\vec{q}) + m_{D^*_{s0}})\right)
\end{aligned} \tag{13}$$

where $V^\mu(|\vec{q}|)$ and $A^\mu(|\vec{q}|)$ $(\mu = 0,3)$ are calculated in our model as

$$\begin{aligned}
V^\mu(|\vec{q}|) &= \left\langle D_s^+,-|\vec{q}|\vec{k}\left|J^{cb\ \mu}_V(0)\right|\bar{B_s},\vec{0}\right\rangle = \sqrt{4m_{\bar{B_s}}E_{D_s}(-\vec{q})}_{\rm NR}\left\langle D_s^+,-|\vec{q}|\vec{k}\left|J^{cb\ \mu}_V(0)\right|\bar{B_s},\vec{0}\right\rangle_{\rm NR}\\
A^\mu(|\vec{q}|) &= \left\langle D^{*+}_{s0},-|\vec{q}|\vec{k}\left|J^{cb\ \mu}_A(0)\right|\bar{B_s},\vec{0}\right\rangle = \sqrt{4m_{\bar{B_s}}E_{D^*_{s0}}(-\vec{q})}_{\rm NR}\left\langle D^{*+}_{s0},-|\vec{q}|\vec{k}\left|J^{cb\ \mu}_A(0)\right|\bar{B_s},\vec{0}\right\rangle_{\rm NR}
\end{aligned} \tag{14}$$

where the expressions for the non-relativistic matrix elements are given in the Appendix. Figure 1 represents the form factors calculated with the wave functions corresponding to the AL1 potential [42].

C. Decays into vector and axial vector states

In the case of decays of $\bar{B_s}$ mesons into vector D_s^{*+} the form factors are given by:

$$\begin{aligned}
V(q^2) &= \frac{i}{\sqrt{2}}\frac{m_{\bar{B_s}}+m_{D_s^*}}{m_{\bar{B_s}}|\vec{q}|}V^1_{\lambda=-1}(|\vec{q}|)\\
A_+(q^2) &= i\frac{m_{\bar{B_s}}+m_{D_s^*}}{2m_{\bar{B_s}}}\frac{m_{D_s^*}}{|\vec{q}|m_{\bar{B_s}}}\left\{-A^0_{\lambda=0}(|\vec{q}|) + \frac{m_{\bar{B_s}}-E_{D_s^*}(-\vec{q})}{|\vec{q}|}A^3_{\lambda=0}(|\vec{q}|) - \sqrt{2}\frac{m_{\bar{B_s}}E_{D_s^*}(-\vec{q})-m^2_{D_s^*}}{|\vec{q}|m_{D_s^*}}A^1_{\lambda=-1}(|\vec{q}|)\right\}\\
A_-(q^2) &= -i\frac{m_{\bar{B_s}}+m_{D_s^*}}{2m_{\bar{B_s}}}\frac{m_{D_s^*}}{|\vec{q}|m_{\bar{B_s}}}\left\{A^0_{\lambda=0}(|\vec{q}|) + \frac{m_{\bar{B_s}}+E_{D_s^*}(-\vec{q})}{|\vec{q}|}A^3_{\lambda=0}(|\vec{q}|) - \sqrt{2}\frac{m_{\bar{B_s}}E_{D_s^*}(-\vec{q})+m^2_{D_s^*}}{|\vec{q}|m_{D_s^*}}A^1_{\lambda=-1}(|\vec{q}|)\right\}\\
A_0(q^2) &= -i\sqrt{2}\frac{1}{m_{\bar{B_s}}-m_{D_s^*}}A^1_{\lambda=-1}(|\vec{q}|)
\end{aligned} \tag{15}$$

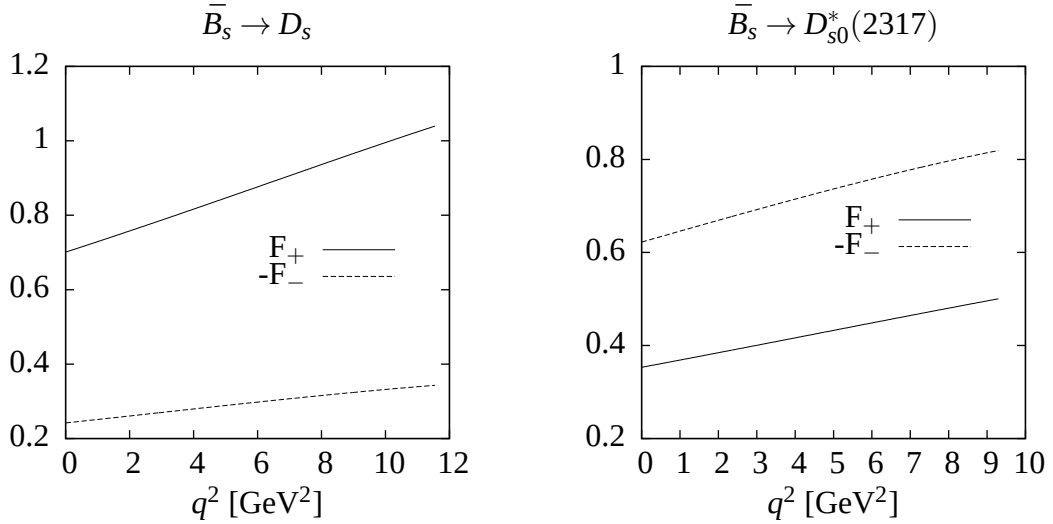

FIG. 1. Form factors for the semileptonic decay of B_s mesons into 0^- (left panel) or 0^+ (right panel) $c\bar{s}$ states.

with $V^\mu_\lambda(|\vec{q}|)$ and $A^\mu_\lambda(|\vec{q}|)$ calculated in our model as

$$V^\mu_\lambda(|\vec{q}|) = \left\langle D_s^{*+}, \lambda - |\vec{q}|\vec{k} \left| J_V^{cb\ \mu}(0) \right| \bar{B_s}, \vec{0} \right\rangle = \sqrt{4 m_{\bar{B_s}} E_{D_s^*}(-\vec{q})}_{\rm NR} \left\langle D_s^{*+}, \lambda - |\vec{q}|\vec{k} \left| J_V^{cb\ \mu}(0) \right| \bar{B_s}, \vec{0} \right\rangle_{\rm NR}$$
$$A^\mu_\lambda(|\vec{q}|) = \left\langle D_s^{*+}, \lambda - |\vec{q}|\vec{k} \left| J_A^{cb\ \mu}(0) \right| \bar{B_s}, \vec{0} \right\rangle = \sqrt{4 m_{\bar{B_s}} E_{D_s^*}(-\vec{q})}_{\rm NR} \left\langle D_s^{*+}, \lambda - |\vec{q}|\vec{k} \left| J_A^{cb\ \mu}(0) \right| \bar{B_s}, \vec{0} \right\rangle_{\rm NR} \quad (16)$$

for which the remaining expressions can be found in the Appendix. The expressions for the axial vectors can be found from those in Eq. (15), by just replacing

$$V^\mu_\lambda(|\vec{q}|) \leftrightarrow -A^\mu_\lambda(|\vec{q}|). \quad (17)$$

Figures 2 and 3 shows the different form factors corresponding to semileptonic decays into vector and pseudovector states. These form factors have been calculated with the wave functions derived from the AL1 potential. In Fig 3, the left (right) panel represents the form factors calculated for semileptonic decays into $^1P_1$ ($^3P_1$) states.

D. Decays into tensor and pseudotensor states

For $\bar{B_s}$ mesons decaying into tensor states, the form factors can be evaluated as

$$T_1(q^2) = -i\frac{2m_{D^*_{s2}}}{m_{\bar{B_s}}|\vec{q}|}A^1_{T\lambda=+1}(|\vec{q}|)$$
$$T_2(q^2) = i\frac{1}{2m^3_{\bar{B_s}}}\left\{-\sqrt{\frac{3}{2}}\frac{m^2_{D^*_{s2}}}{|\vec{q}|^2}A^0_{T\lambda=0}(|\vec{q}|) - \sqrt{\frac{3}{2}}\frac{m^2_{D^*_{s2}}}{|\vec{q}|^3}(E_{D^*_{s2}}(-\vec{q}) - m_{\bar{B_s}})A^3_{T\lambda=0}(|\vec{q}|) + \frac{2m_{D^*_{s2}}}{|\vec{q}|}\left(1 - \frac{E_{D^*_{s2}}(-\vec{q})}{|\vec{q}|^2}(E_{D^*_{s2}}(-\vec{q}) - m_{\bar{B_s}})\right)\right\}$$
$$T_3(q^2) = i\frac{1}{2m^3_{\bar{B_s}}}\left\{-\sqrt{\frac{3}{2}}\frac{m^2_{D^*_{s2}}}{|\vec{q}|^2}A^0_{T\lambda=0}(|\vec{q}|) - \sqrt{\frac{3}{2}}\frac{m^2_{D^*_{s2}}}{|\vec{q}|^3}(E_{D^*_{s2}}(-\vec{q}) + m_{\bar{B_s}})A^3_{T\lambda=0}(|\vec{q}|) + \frac{2m_{D^*_{s2}}}{|\vec{q}|}\left(1 - \frac{E_{D^*_{s2}}(-\vec{q})}{|\vec{q}|^2}(E_{D^*_{s2}}(-\vec{q}) + m_{\bar{B_s}})\right)\right\}$$
$$T_4(q^2) = i\frac{m_{D^*_{s2}}}{m^2_{\bar{B_s}}|\vec{q}|^2}A^1_{T\lambda=+1}(|\vec{q}|) \quad (18)$$

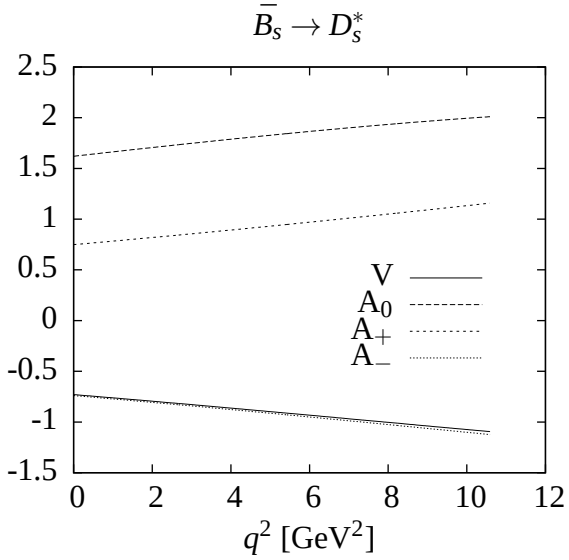

FIG. 2. Form factors for the decay of B_s mesons into vector D_s^* states.

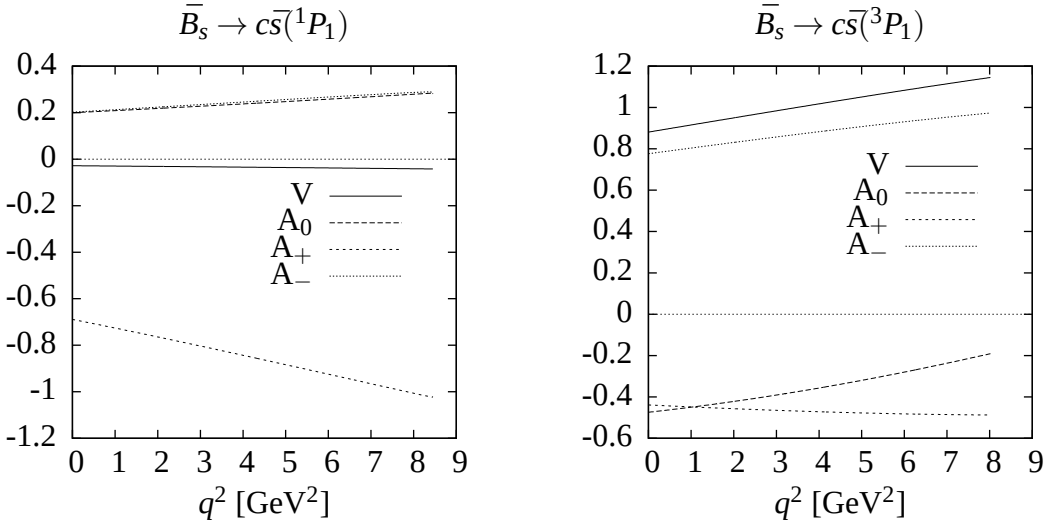

FIG. 3. Form factors for the decay of B_S mesons into $c\bar{s}, J^P = 1^+, S = 0$ (left panel) and $c\bar{s}, J^P = 1^+, S = 1$ (right panel) states.

with $V^\mu_{T\lambda}(|\vec{q}|)$ and $A^\mu_{T\lambda}(|\vec{q}|)$ calculated in our model as

$$V^\mu_{T\lambda}(|\vec{q}|) = \left\langle D_{s2}^{*+}, \lambda - |\vec{q}|\vec{k} \left| J_V^{cb\,\mu}(0) \right| \bar{B_s}, \vec{0} \right\rangle = \sqrt{4m_{\bar{B_s}} E_{D_{s2}^*}(-\vec{q})}_{\rm NR} \left\langle D_{s2}^{*+}, \lambda - |\vec{q}|\vec{k} \left| J_V^{cb\,\mu}(0) \right| \bar{B_s}, \vec{0} \right\rangle_{\rm NR}$$

$$A^\mu_{T\lambda}(|\vec{q}|) = \left\langle D_{s2}^{*+}, \lambda - |\vec{q}|\vec{k} \left| J_A^{cb\,\mu}(0) \right| \bar{B_s}, \vec{0} \right\rangle = \sqrt{4m_{\bar{B_s}} E_{D_{s2}^*}(-\vec{q})}_{\rm NR} \left\langle D_{s2}^{*+}, \lambda - |\vec{q}|\vec{k} \left| J_A^{cb\,\mu}(0) \right| \bar{B_s}, \vec{0} \right\rangle_{\rm NR} \quad (19)$$

for which the remaining expressions can be found in the Appendix. Again, the form factor corresponding to a decay into a pseudotensor state can be obtained from those above, just replacing

$$V^\mu_{T\lambda}(|\vec{q}|) \leftrightarrow -A^\mu_{T\lambda}(|\vec{q}|). \quad (20)$$

In Figure 4 we have represented the form factors corresponding to decays into tensor and pseudotensor states, with the wave functions of the AL1 potential.

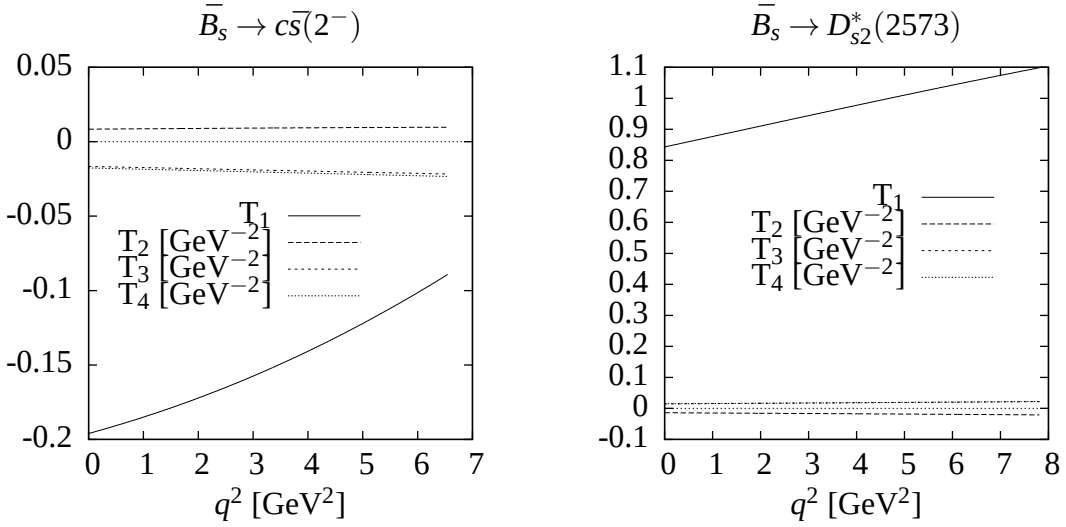

FIG. 4. Form factors for the decay of B_s mesons into tensor (left panel) and pseudotensor (right panel) $c\bar{s}$ states.

E. Decay width

Let us consider the double differential decay width with respect to q^2 and the cosine, x_l, of the angle between the final meson momentum and the momentum of the final charged lepton, the latter measured in the lepton-neutrino center of mass frame (CMF). For a $\bar{B_s}$ at rest, this differential decay width results to be

$$\frac{d^2\Gamma}{dx_l dq^2} = \frac{G_F^2}{64m^2_{\bar{B_s}}} \frac{|V_{bc}|^2}{8\pi^3} \frac{\lambda^{1/2}(q^2, m^2_{\bar{B_s}}, m^2_{c\bar{s}})}{2m_{\bar{B_s}}} \frac{q^2 - m_l^2}{q^2} \mathcal{H}_{\alpha\beta}(P_{\bar{B_s}}, P_{c\bar{s}}) \mathcal{L}^{\alpha\beta}(p_l, p_\nu), \tag{21}$$

where $G_F = 1.16637(1) \times 10^{-5}\text{GeV}^{-2}$ [39] is the Fermi constant, $\lambda(a,b,c) = (a+b-c)^2 - 4ab$, m_l is the mass of the charged lepton, $\mathcal{H}$ and $\mathcal{L}$ are the hadron and lepton tensors, and $P_{\bar{B_s}}$, $P_{c\bar{s}}$, p_l and p_ν are the meson and lepton four momenta.

The lepton tensor is

$$\mathcal{L}^{\alpha\beta}(p_l, p_\nu) = 8(p_l^\alpha p_\nu^\beta + p_l^\beta p_\nu^\alpha - g^{\alpha\beta} p_l \cdot p_\nu \mp i\varepsilon^{\alpha\beta\sigma\rho} p_{l\sigma} p_{\nu\rho}) \tag{22}$$

where, in the last term, the minus (plus) sign corresponds to a decay into $l^-\bar{\nu}_l$ ($l^+\nu_l$). The hadron tensor is given by

$$\mathcal{H}_{\alpha\beta} = \sum_\lambda h_{(\lambda)\alpha}(P_{\bar{B_s}}, P_{c\bar{s}}) h^{(*)}_{(\lambda)\beta}(P_{\bar{B_s}}, P_{c\bar{s}}) \tag{23}$$

where

$$h_{(\lambda)\alpha}(P_{\bar{B_s}}, P_{c\bar{s}}) = \left\langle c\bar{s}, \lambda \vec{P}_{c\bar{s}} \middle| J^{cb}_\alpha \middle| \bar{B_s} \vec{P}_{\bar{B_s}} \right\rangle. \tag{24}$$

is just the corresponding matrix element of the $b \to c$ V-A weak current given in Eq. 8.

To evaluate the scalar

$$\mathcal{H}_{\alpha\beta}(P_{\bar{B_s}}, P_{c\bar{s}}) \mathcal{L}^{\alpha\beta}(p_l, p_\nu) \tag{25}$$

we choose $\vec{P}_{c\bar{s}}$ to be along the negative $z-$axis, which involves that the lepton CMF moves along the positive $z-$axis.

To proceed with the calculation we shall follow [38] and introduce the helicity components for the hadron and lepton tensor and rewrite the scalar of the expression of Eq. (25) as

$$\mathcal{H}_{\alpha\beta}(P_{\bar{B}_s},P_{c\bar{s}})\mathcal{L}^{\alpha\beta}(p_l,p_\nu)=\mathcal{H}^{\sigma\rho}(P_{\bar{B}_s},P_{c\bar{s}})g_{\sigma\alpha}g_{\beta\rho}\mathcal{L}^{\alpha\beta}(p_l,p_\nu) \tag{26}$$

where [43]

$$\begin{aligned} g_{\mu\nu}&=\sum_{r=t,\pm1,0} g_{rr}\varepsilon_{(r)\mu}(q)g_{rr}\varepsilon^{(*)}_{(r)\nu}(q)\\ g_{tt}&=1,\ \ g_{\pm1,0}=-1 \end{aligned} \tag{27}$$

with $\varepsilon^{\mu}_{(t)}(q)=q^\mu/q^2$ and $\varepsilon_{(r)}(q),\ r=\pm1,0$ are the polarization vector for an on-shell particle with four momentum q and polarization r.

We shall define the helicity components of the hadron and lepton tensors as

$$\begin{aligned} \mathcal{H}_{rs}(P_{\bar{B}_s},P_{c\bar{s}})&=\varepsilon^*_{(r)\sigma}(q)\mathcal{H}^{\sigma\rho}(P_{\bar{B}_s},P_{c\bar{s}})\varepsilon_{(s)\rho}(q)\\ \mathcal{L}_{rs}(p_l,p_\nu)&=\varepsilon_{(r)\sigma}(q)\mathcal{L}^{\sigma\rho}(p_l,p_\nu)\varepsilon^*_{(s)\rho}(q). \end{aligned} \tag{28}$$

The contraction of lepton and hadron tensors is, using the expressions above

$$\mathcal{H}_{\alpha\beta}(P_{\bar{B}_s},P_{c\bar{s}})\mathcal{L}^{\alpha\beta}(p_l,p_\nu)=\sum_{r,s=t,\pm1,0} g_{rr}g_{ss}\mathcal{H}_{rs}(P_{\bar{B}_s},P_{c\bar{s}})\mathcal{L}_{rs}(p_l,p_\nu) \tag{29}$$

We take advantage of the fact that the Wigner rotation relating the original frame and the CMF of the final leptons is the identity. In the latter, we have

$$\mathcal{L}_{rs}(p_l,p_\nu)=\varepsilon_{(r)\alpha}(q)\mathcal{L}^{\alpha\beta}(p_l,p_\nu)\varepsilon_{(s)\beta}(q)=\varepsilon_{(r)\alpha}(\tilde{q})\mathcal{L}^{\alpha\beta}(\tilde{p}_l,\tilde{p}_\nu)\varepsilon_{(s)\beta}(\tilde{q}) \tag{30}$$

where the tilde stands for the momentum measured in the leptons CMF. For evaluation, we take[2]

$$\begin{aligned} \tilde{p}^\alpha_l&=(E_l(|\tilde{p}_l|),|\tilde{p}_l|\sqrt{(1-x_l^2)},0,|\tilde{p}_l|x_l)\\ \tilde{p}^\alpha_\nu&=(|\tilde{p}_l|,|\tilde{p}_l|\sqrt{(1-x_l^2)},0,|\tilde{p}_l|x_l) \end{aligned} \tag{31}$$

where $|\tilde{p}_l|$ is the modulus of the lepton three momentum in the leptons CMF. Now let us evaluate the lepton tensor helicity components that we need.

$$\begin{aligned} \mathcal{L}_{tt}(p_l,p_\nu)&=4\frac{m_l^2(q^2-m^2)}{q^2}\\ \mathcal{L}_{t0}(p_l,p_\nu)&=-4x_l\frac{m_l^2(q^2-m^2)}{q^2}\\ \mathcal{L}_{+1+1}(p_l,p_\nu)&=(q^2-m^2)\left(4(1\pm x_l)-2(1-x_l^2)\frac{(q^2-m^2)}{q^2}\right)\\ \mathcal{L}_{-1-1}(p_l,p_\nu)&=(q^2-m^2)\left(4(1\mp x_l)-2(1-x_l^2)\frac{(q^2-m^2)}{q^2}\right)\\ \mathcal{L}_{00}(p_l,p_\nu)&=4(q^2-m^2)\frac{1-x_l(q^2-m^2)}{q^2} \end{aligned} \tag{32}$$

As for the hadron tensor, we introduce the helicity amplitudes defined as

$$h_{(\lambda)r}(P_{\bar{B}_s},P_{c\bar{s}})=\varepsilon^*_{(r)\alpha}h^\alpha_{(\lambda)}(P_{\bar{B}_s},P_{c\bar{s}}), \tag{33}$$

in terms of which the hadron tensor can be written as

$$\mathcal{H}_{rs}(P_{\bar{B}_s},P_{c\bar{s}})=\sum_\lambda h_{(\lambda)r}(P_{\bar{B}_s},P_{c\bar{s}})h^*_{(\lambda)s}(P_{\bar{B}_s},P_{c\bar{s}}) \tag{34}$$

---

[2] As we have taken the momentum of the final meson in the negative z direction, this is in accordance with the definition of x_l.

The expressions for the helicity amplitudes in the original frame are given as [38, 40]:

- Transitions to scalar states

$$\begin{aligned} h_t(P_{\bar{B}_s},P_{c\bar{s}}) &= \frac{m^2_{\bar{B}_s}-m^2_{c\bar{s}}}{\sqrt{q^2}}F_+(q^2)+\sqrt{q^2}F_-(q^2) \\ h_0(P_{\bar{B}_s},P_{c\bar{s}}) &= \frac{\lambda^{1/2}(q^2,m^2_{\bar{B}_s},m^2_{c\bar{s}})}{\sqrt{q^2}}F_+(q^2) \\ h_{+1}(P_{\bar{B}_s},P_{c\bar{s}}) &= h_{-1}(P_{\bar{B}_s},P_{c\bar{s}}) = 0 \end{aligned} \tag{35}$$

- Transitions to vector states

$$\begin{aligned} h_{(\lambda)t}(P_{\bar{B}_s},P_{c\bar{s}}) &= i\delta_{\lambda 0}\frac{\lambda^{1/2}(q^2,m^2_{\bar{B}_s},m^2_{c\bar{s}})}{2m_{c\bar{s}}\sqrt{q^2}}\left((m_{\bar{B}_s}-m_{c\bar{s}})(A_0(q^2)-A_+(q^2))-\frac{q^2}{m_{\bar{B}_s}+m_{c\bar{s}}}A_-(q^2)\right) \\ h_{(\lambda)+1}(P_{\bar{B}_s},P_{c\bar{s}}) &= -i\delta_{\lambda-1}\left(\frac{\lambda^{1/2}(q^2,m^2_{\bar{B}_s})}{m_{\bar{B}_s}+m_{c\bar{s}}}V(q^2)+(m_{\bar{B}_s}-m_{c\bar{s}})A_0(q^2)\right) \\ h_{(\lambda)-1}(P_{\bar{B}_s},P_{c\bar{s}}) &= -i\delta_{\lambda+1}\left(\frac{\lambda^{1/2}(q^2,m^2_{\bar{B}_s})}{m_{\bar{B}_s}+m_{c\bar{s}}}V(q^2)+(m_{\bar{B}_s}-m_{c\bar{s}})A_0(q^2)\right) \\ h_{(\lambda)0}(P_{\bar{B}_s},P_{c\bar{s}}) &= i\delta_{\lambda 0}\left((m_{\bar{B}_s}-m_{c\bar{s}})\frac{m^2_{\bar{B}_s}-q^2-m^2_{c\bar{s}}}{2m_{c\bar{s}}\sqrt{q^2}}A_0(q^2)-\frac{\lambda(q^2,m^2_{\bar{B}_s},m^2_{c\bar{s}})}{2m_{c\bar{s}}\sqrt{q^2}}\frac{A_+(q^2)}{m_{\bar{B}_s}+m_{c\bar{s}}}\right) \end{aligned} \tag{36}$$

- Transitions to tensor states

$$\begin{aligned} h_{(\lambda)t}(P_{\bar{B}_s},P_{c\bar{s}}) &= -i\delta_{\lambda 0}\sqrt{\frac{2}{3}}\frac{\lambda(q^2,m^2_{\bar{B}_s},m^2_{c\bar{s}})}{4m^2_{c\bar{s}}\sqrt{q^2}}\left(T_1(q^2)+(m^2_{\bar{B}_s}-m^2_{c\bar{s}})T_2(q^2)+q^2T_3(q^2)\right) \\ h_{(\lambda)+1}(P_{\bar{B}_s},P_{c\bar{s}}) &= i\delta_{\lambda-1}\frac{1}{\sqrt{2}}\frac{\lambda^{1/2}(q^2,m^2_{\bar{B}_s},m^2_{c\bar{s}})}{2m_{c\bar{s}}}\left(T_1(q^2)-\lambda^{1/2}(q^2,m^2_{\bar{B}_s}m^2_{c\bar{s}})T_4(q^2)\right) \\ h_{(\lambda)-1}(P_{\bar{B}_s},P_{c\bar{s}}) &= i\delta_{\lambda+1}\frac{1}{\sqrt{2}}\frac{\lambda^{1/2}(q^2,m^2_{\bar{B}_s},m^2_{c\bar{s}})}{2m_{c\bar{s}}}\left(T_1(q^2)+\lambda^{1/2}(q^2,m^2_{\bar{B}_s}m^2_{c\bar{s}})T_4(q^2)\right) \\ h_{(\lambda)0}(P_{\bar{B}_s},P_{c\bar{s}}) &= -i\delta_{\lambda 0}\sqrt{\frac{2}{3}}\frac{\lambda^{1/2}(q^2,m^2_{\bar{B}_s},m^2_{c\bar{s}})}{4m^2_{c\bar{s}}\sqrt{q^2}}\left((m^2_{\bar{B}_s}-q^2-m_{c\bar{s}})T_1(q^2)+\lambda(q^2,m^2_{\bar{B}_s},m^2_{c\bar{s}})T_2(q^2)\right) \end{aligned} \tag{37}$$

Where we shall remark that the helicity amplitudes, and thus the components of the hadron tensor depend only on q^2. We define the following combinations for further convenience:

$$\begin{aligned} H_U &= \mathcal{H}_{+1+1}+\mathcal{H}_{-1-1} \\ H_P &= \mathcal{H}_{+1+1}-\mathcal{H}_{-1-1} \\ H_L &= \mathcal{H}_{00};\ H_S = 3\mathcal{H}_{tt};\ H_{SL} = \mathcal{H}_{t0} \\ \tilde{H}_J &= \frac{m_l^2}{2q^2}\mathcal{H};\ \ J = U,L,S,SL \end{aligned} \tag{38}$$

with U, L, P, S and SL representing, respectively, unpolarized-transverse, longitudinal, parity-odd, scalar and scalar-longitudinal interference.

The double differential decay width can be written in terms of the combination above as

$$\begin{aligned} \frac{d^2\Gamma}{dq^2dx_l} &= \frac{G_F^2}{8\pi^3}|V_{bc}|^2\frac{(q^2-m_l^2)^2}{12m^2_{\bar{B}_s}q^2}\frac{\lambda^{1/2}(q^2,m^2_{\bar{B}_s},m^2_{c\bar{s}})}{2m_{\bar{B}_s}} \\ &\times\left\{\frac{3}{8}(1+x_l^2)H_U+\frac{3}{4}(1-x_l^2)H_L\pm\frac{3}{4}H_P+\frac{3}{4}(1-x_l^2)\tilde{H}_U+\frac{3}{2}x_l^2\tilde{H}_l+\frac{1}{2}\tilde{H}_S+3x_l\tilde{H}_{sl}\right\} \end{aligned} \tag{39}$$

The term H_P changes sign for antiparticle decay, in contrast to the rest of the helicity components. This extra sign compensates the $\mp$ sign in the lepton tensor, leading to an expression for the double differential decay which is the same for particle or antiparticle decay.

Finally, we obtain the differential decay width integrating over x_l.

$$\frac{d\Gamma}{dq^2} = \frac{G_F^2}{8\pi^3}|V_{bc}|^2 \frac{(q^2-m_l^2)^2}{12 m_{\bar{B}_s}^2 q^2} \frac{\lambda^{1/2}(q^2, m_{\bar{B}_s}^2, m_{c\bar{s}}^2)}{2m_{\bar{B}_s}} \left\{ H_U + H_L + \tilde{H}_U + \tilde{H}_L + \tilde{H}_S \right\}, \tag{40}$$

from where we obtain the total decay width integrating over q^2, that can be written as

$$\Gamma = \Gamma_U + \Gamma_L + \tilde{\Gamma}_U + \tilde{\Gamma}_L + \tilde{\Gamma}_S, \tag{41}$$

with Γ and Γ_J partial helicity widths defined as

$$\Gamma_J = \int dq^2 \frac{G_F^2}{8\pi^3}|V_{bc}|^2 \frac{(q^2-m_l^2)^2}{12 m_{\bar{B}_s}^2 q^2} \frac{\lambda^{1/2}(q^2, m_{\bar{B}_s}^2, m_{c\bar{s}}^2)}{2m_{\bar{B}_s}} H_J \tag{42}$$

and similarly for $\tilde{\Gamma}_J$ in terms of $\tilde{H}_J$.

The forward-backward asymmetry of the charged leptons, measured in the leptons CMF, which in terms of partial helicity widths, can be written as

$$A_{FB} = \frac{\Gamma_{x_l>0} - \Gamma_{x_l<0}}{\Gamma_{x_l>0} + \Gamma_{x_l<0}} = \frac{3}{4} \frac{\pm\Gamma_P + 4\tilde{\Gamma}_{SL}}{\Gamma_U + \Gamma_L + \tilde{\Gamma}_U + \tilde{\Gamma}_L + \tilde{\Gamma}_S} \tag{43}$$

As Γ_P changes sign for antiparticle decay, A_{FB} is the same for a negative charged lepton as for a positive.

F. Results

Table III summarizes the values for the total decay widths calculated with our model. We give the semileptonic decay widths for the different leptons in the final state, in units of 10^{-15}GeV. The central values have been calculated using the AL1 potential of [42], while the theoretical uncertainties have been estimated by considering other potential models (see Ref. [42]). Table IV shows the corresponding values for branching fractions.

In Table V we compare with previous results. In Refs. [28] the authors adopt the relativistic quark model. Chen *et al.* solve the instantaneous Bethe-Salpeter equation in [32] to estimate the weak transition form factors. In [33] the authors work out the form factors within the covariant light front quark model. Azizi *et al.* in [34, 35] and Blasi *et al.* in [36] apply the sum rules technique to obtain the form factors and branching fractions. In [37], work within the Constituent Quark Model, as in this work. In Ref. [44] we studied some of the decays into orbitally excited final D_s states, using the potential model of [45].

The results of this work are in a systematic good agreement with those from the relativistic quark model of [28]. The agreement is also good with the quark model calculation of [37]. It is worth to mention that our results for decays into orbitally excited final D_s mesons are in rather good agreement with our previous results from [44], though in that work the potential model that have been used is much more sophisticated, even enabling the posibility to consider non-$q\bar{q}$ components for these orbitally excited states. Our results also compare well to the sum-rules calculation of [34, 35], while the result of [36] is lower by about one half. The same happens if we compare with the results of [32] or [33].

In Tables VI and VII we give our results for partial helicity widths corresponding to $\bar{B}_s^0$, and the values we obtain for the forward-backward asymetry, respectively. In Table VI the "P" column changes sign for B_s^0 decay. As before, the central values have been evaluated with the AL1 potential.

In the different panels of Figures 5 to 8 we plot the differential decay widths that we obtain for the different J^P $c\bar{s}$ final states, with e^+ or τ^+, accounting for the leptons.

G. Heavy Quark Symmetry

In systems with a quark with mass much larger than the QCD scale ($\Lambda_{\rm QCD}$), the dynamics of the light degrees of freedom becomes independent of the heavy quark flavor and spin.

$\bar{B_S} \to M' l^- \bar{\nu}_l$	$\Gamma[10^{-15}\text{GeV}]$		
M'	$l = e$	$l = \mu$	$l = \tau$
D_s^+	$10.37^{+0.15}_{-0.2}$	$10.32^{+0.16}_{-0.10}$	$2.99^{+0.01}_{-0.03}$
D_{s0}^{*+}	$1.75^{+0.03}_{-0.07}$	$1.74^{+0.03}_{-0.08}$	$0.20^{+0.003}_{-0.003}$
D_s^{*+}	$28.02^{+0.24}_{-0.48}$	$27.90^{+0.86}_{-0.48}$	$6.86^{+0.12}_{-0.09}$
$D_{s1}^+(2460)$	$2.07_{-0.09}$	$2.05_{-0.08}$	$0.17_{-0.008}$
$D_{s1}^+(2536)$	$1.40_{-0.07}$	$1.39_{-0.07}$	$0.12_{-0.006}$
$c\bar{s}(2^-)$	$4.11_{-0.56}\ 10^{-2}$	$4.06_{-0.64}\ 10^{-2}$	$9.02_{-2.39}\ 10^{-4}$
D_{s2}^{*+}	$1.97_{-0.15}$	$1.95_{-0.14}$	$0.12_{-0.02}$

TABLE III. Decay widths in units of 10^{-15} GeV for semileptonic $\bar{B_s} \to c\bar{s}$ decays. The central value has been obtained with the AL1 potential.

M'	$l = e, \mu$	$l = \tau$
D_s^+	2.32	0.67
D_{s0}^{*+}	0.39	0.04
D_s^{*+}	6.26	1.53
$D_{s1}^+(2460)$	0.47	0.04
$D_{s1}^+(2536)$	0.32	0.03
$c\bar{s}(2^-)$	$9.2\ 10^{-3}$	$2.0\ 10^{-4}$
D_{s2}^{*+}	0.44	0.03

TABLE IV. Branching fractions for the indicated decay channels, in percentage.

The six form factors involved in the $\bar{B_s}$ decays into pseudoscalar and vector mesons are related by HQS, which reduces their evaluation to that of a single function, ξ. In particular, HQS predicts [20, 21]:

$$\begin{aligned} h_+(\omega) &= h_V(\omega) = h_{A_1}(\omega) = h_{A_3}(\omega) = \xi(\omega) \\ h_-(\omega) &= h_{A_2}(\omega) = 0. \end{aligned} \tag{44}$$

The h form factors are just a redefinition of the those above, given by

$$h_\pm(\omega) = \frac{2m_{\bar{B_s}}}{\sqrt{2m_{\bar{B_s}} m_{c\bar{s}}}} f_\pm(\omega) \tag{45}$$

	This work	[28]	[32]	[33]	[36]	[37]	[34],[35]	[44]
$\bar{B_s} \to D_s^+ e^- \bar{\nu}_e$	2.32	2.1 ± 0.2	1.4-1.7	$1.0^{+0.4}_{-0.3}$	1.35 ± 0.21	2.73-3.00	2.8-3.8	
$\bar{B_s} \to D_s^{*+} e^- \bar{\nu}_e$	6.26	5.3 ± 0.5	5.1-5.8		2.5 ± 0.1	7.49-7.66	1.89-6.61	
$\bar{B_s} \to D_s^+ \tau^- \bar{\nu}_\tau$	0.67	0.62 ± 0.05	0.47-0.55	$0.33^{+0.14}_{-0.11}$				
$\bar{B_s} \to D_s^{*+} \tau^- \bar{\nu}_\tau$	1.53	1.3 ± 0.1	1.2-1.3					
$\bar{B_s} \to D_{s0}^{*+} \mu^- \bar{\nu}_\mu$	0.39							0.44
$\bar{B_s} \to D_{s1}^{*+}(2460) \mu^- \bar{\nu}_\mu$	0.47							0.17-0.5
$\bar{B_s} \to D_{s1}^{*+}(2536) \mu^- \bar{\nu}_\mu$	0.32							0.4
$\bar{B_s} \to D_{s2}^{*+} \mu^- \bar{\nu}_\mu$	0.44							0.37

TABLE V. Branching fractions for the indicated decay channels, in percentage.

	Γ_U	$\tilde{\Gamma}_U$	Γ_L	$\tilde{\Gamma}_L$	Γ_P	$\tilde{\Gamma}_S$	$\tilde{\Gamma}_{SL}$
$\bar{B_s} \to D_s^+ e^- \bar{\nu}_e$	0	0	10.37	$2.29\ 10^{-6}$	0	$7.43\ 10^{-6}$	$2.36\ 10^{-6}$
$\bar{B_s} \to D_{s0}^{*+} e^- \bar{\nu}_e$	0	0	1.75	$4.82\ 10^{-7}$	0	$1.44\ 10^{-6}$	$4.81\ 10^{-7}$
$\bar{B_s} \to D_s^{*+} e^- \bar{\nu}_e$	13.87	$4.15\ 10^{-7}$	14.16	$2.13\ 10^{-6}$	-7.32	$5.90\ 10^{-6}$	$2.03\ 10^{-6}$
$\bar{B_s} \to D_{s1}^+(2460) e^- \bar{\nu}_e$	0.32	$1.6\ 10^{-8}$	1.75	$6.41\ 10^{-7}$	-0.22	$1.98\ 10^{-6}$	$6.51\ 10^{-7}$
$\bar{B_s} \to D_{s1}^+(2536) e^- \bar{\nu}_e$	0.56	$2.97\ 10^{-8}$	0.84	$3.04\ 10^{-7}$	-0.44	$9.40\ 10^{-7}$	$3.08\ 10^{-7}$
$\bar{B_s} \to c\bar{s}(2^-) e^- \bar{\nu}_e$	$3.95\ 10^{-2}$	$3.37\ 10^{-9}$	$1.58\ 10^{-3}$	$3.55\ 10^{-10}$	$-3.24\ 10^{-2}$	$8.76\ 10^{-10}$	$3.15\ 10^{-10}$
$\bar{B_s} \to D_{s2}^{*+} e^- \bar{\nu}_e$	0.67	$3.76\ 10^{-8}$	1.30	$4.35\ 10^{-7}$	-0.35	$1.25\ 10^{-6}$	$4.24\ 10^{-7}$
$\bar{B_s} \to D_s^+ \mu^- \bar{\nu}_\mu$	0	0	10.11	$4.72\ 10^{-2}$	0	0.16	$5.05\ 10^{-2}$
$\bar{B_s} \to D_{s0}^{*+} \mu^- \bar{\nu}_\mu$	0	0	1.70	$9.47\ 10^{-3}$	0	$2.80\ 10^{-2}$	$9.40\ 10^{-3}$
$\bar{B_s} \to D_s^{*+} \mu^- \bar{\nu}_\mu$	13.80	$1.74\ 10^{-2}$	13.91	$4.68\ 10^{-2}$	-7.28	0.12	$4.28\ 10^{-2}$
$\bar{B_s} \to D_{s1}^+(2460) \mu^- \bar{\nu}_\mu$	0.32	$6.6\ 10^{-4}$	1.68	$1.7\ 10^{-2}$	-0.21	$3.79\ 10^{-2}$	$1.22\ 10^{-2}$
$\bar{B_s} \to D_{s1}^+(2536) \mu^- \bar{\nu}_\mu$	0.55	$1.23\ 10^{-3}$	0.81	$5.58\ 10^{-3}$	-0.44	$1.79\ 10^{-3}$	$5.76\ 10^{-3}$
$\bar{B_s} \to c\bar{s}(2^-) \mu^- \bar{\nu}_\mu$	$3.89\ 10^{-2}$	$1.37\ 10^{-4}$	$1.55\ 10^{-3}$	$7.49\ 10^{-6}$	$-3.20\ 10^{-2}$	$1.46\ 10^{-5}$	$5.82\ 10^{-6}$
$\bar{B_s} \to D_{s2}^{*+} \mu^- \bar{\nu}_\mu$	0.66	$1.55\ 10^{-3}$	1.26	$8.15\ 10^{-3}$	-0.35	$2.20\ 10^{-2}$	$7.69\ 10^{-3}$
$\bar{B_s} \to D_s^+ \tau^- \bar{\nu}_\tau$	0	0	0.94	0.22	0	1.82	0.36
$\bar{B_s} \to D_{s0}^{*+} \tau^- \bar{\nu}_\tau$	0	0	$9.28\ 10^{-2}$	$2.51\ 10^{-2}$	0	$8.26\ 10^{-2}$	$2.61\ 10^{-2}$
$\bar{B_s} \to D_s^{*+} \tau^- \bar{\nu}_\tau$	3.18	0.68	2.06	0.46	-1.39	0.49	0.26
$\bar{B_s} \to D_{s1}^+(2460) \tau^- \bar{\nu}_\tau$	0.03	$8.22\ 10^{-3}$	$5.19\ 10^{-2}$	$1.50\ 10^{-2}$	$-1.71\ 10^{-2}$	0.07	$1.88\ 10^{-2}$
$\bar{B_s} \to D_{s1}^+(2536) \tau^- \bar{\nu}_\tau$	$4.48\ 10^{-2}$	$1.25\ 10^{-2}$	$2.60\ 10^{-2}$	$7.49\ 10^{-3}$	$-3.39\ 10^{-2}$	$3.53\ 10^{-2}$	$8.96\ 10^{-3}$
$\bar{B_s} \to c\bar{s}(2^-) \tau^- \bar{\nu}_\tau$	$6.26\ 10^{-4}$	$2.14\ 10^{-4}$	$4.42\ 10^{-5}$	$1.44\ 10^{-5}$	$-5.34\ 10^{-4}$	$3.05\ 10^{-8}$	$3.68\ 10^{-6}$
$\bar{B_s} \to D_{s2}^{*+} \tau^- \bar{\nu}_\tau$	$4.26\ 10^{-2}$	$1.25\ 10^{-2}$	$3.85\ 10^{-2}$	$1.15\ 10^{-2}$	$-1.75\ 10^{-2}$	$1.22\ 10^{-2}$	$6.73\ 10^{-3}$

TABLE VI. Partial helicity widths in units of 10^{-15} GeV. These results have been calculated using the AL1 potential.

	$A_{\rm FB}$		
	$l = e$	$l = \mu$	$l = \tau$
$\bar{B_s} \to D_s^+ l^- \bar{\nu}_l$	$6.86\ 10^{-7}$	$1.47\ 10^{-2}$	0.36
$\bar{B_s} \to D_{s0}^{*+} l^- \bar{\nu}_l$	$8.22\ 10^{-7}$	$1.62\ 10^{-2}$	0.39
$\bar{B_s} \to D_s^{*+} l^- \bar{\nu}_l$	-0.20	-0.19	$-3.71\ 10^{-2}$
$\bar{B_s} \to D_{s1}^+(2460) l^- \bar{\nu}_l$	-0.19	-0.18	0.10
$\bar{B_s} \to D_{s1}^+(2536) l^- \bar{\nu}_l$	-0.41	-0.40	-0.20
$\bar{B_s} \to c\bar{s}(2^-) l^- \bar{\nu}_l$	-0.59	-0.59	-0.43
$\bar{B_s} \to D_{s2}^{*+} l^- \bar{\nu}_l$	-0.14	-0.12	$6.03\ 10^{-2}$

TABLE VII. Forward-Backward asymmetry parameters for the semileptonic B_s decays, obtained for the AL1 potential.

for decays into pseudoscalar states, and

$$
\begin{aligned}
h_V(\omega) &= \sqrt{2}\sqrt{\frac{M_{D_s^*}}{M_{\bar{B_s}}}}\frac{V^2_{\lambda=-1}(|\vec{q}|)}{|\vec{q}|} \\
h_{A_1}(\omega) &= i\frac{\sqrt{2}}{w+1}\frac{1}{\sqrt{M_{\bar{B_s}} M_{D_s^*}}} A^1_{\lambda=-1}(|\vec{q}|) \\
h_{A_2}(\omega) &= i\sqrt{\frac{M_{D_s^*}}{M_{\bar{B_s}}}}\left(-\frac{A^0_{\lambda=0}(|\vec{q}|)}{|\vec{q}|} + \frac{E_{D_s^*}(|\vec{q}|)A^3_{\lambda=0}(|\vec{q}|)}{|\vec{q}|^2} - \sqrt{2}M_{D^*}\frac{A^1_{\lambda=-1}(|\vec{q}|)}{|\vec{q}|^2}\right) \\
h_{A_3}(\omega) &= i\frac{M^2_{D_s^*}}{\sqrt{M_{D_s^*} M_{\bar{B_s}}}}\left(-\frac{A^3_{\lambda=0}(|\vec{q}|)}{|\vec{q}|^2} + \frac{\sqrt{2}}{M_{D^*}}\frac{A^1_{\lambda=-1}(|\vec{q}|)}{|\vec{q}|^2}\right)
\end{aligned}
\tag{46}
$$

for decays into vector states [23].

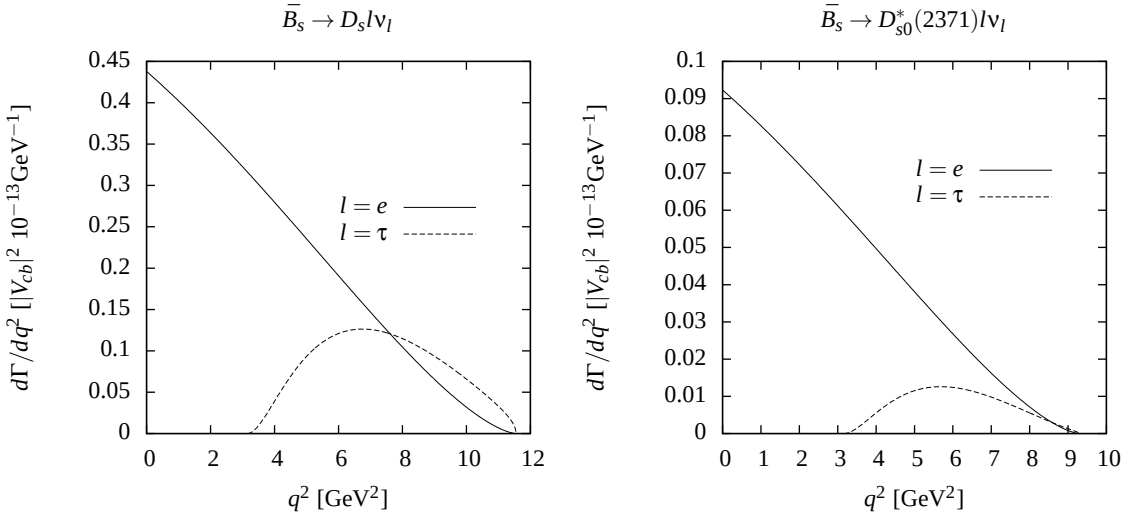

FIG. 5. Differential decay width for the $\bar{B_s}$ into 0^- (left panel) and 0^+ (right panel) states.

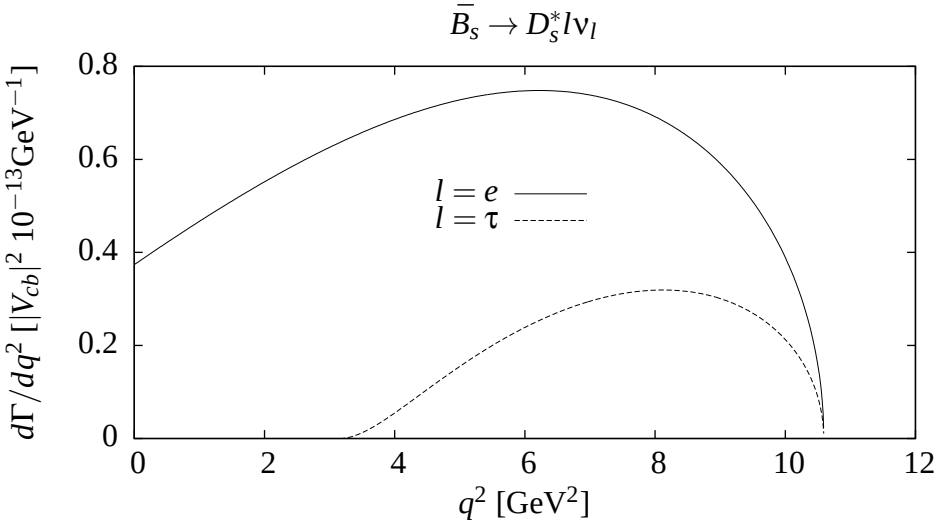

FIG. 6. Differential decay width for the semileptonic $\bar{B_s} \to D^*$ process.

Conservation of vector current in the equal mass case, provides another constrain, in the form of a normalization condition:

$$\xi(\omega = 1) = 1. \tag{47}$$

The purpose of this section is test the form factors we have obtained previously against the HQS predictions. In the left panel of Fig. 9 we plot our values for the h form factors. These values have been obtained with the wave functions of the AL1 potential. In the right panel of Fig. 9, we also evaluate the ratios

$$\begin{aligned} R_1(\omega) &= \frac{h_V(\omega)}{h_{A_1}(\omega)} \\ R_2(\omega) &= \frac{h_{A_3}(\omega) + r h_{A_2}(\omega)}{h_{A_1}(\omega)} \end{aligned} \tag{48}$$

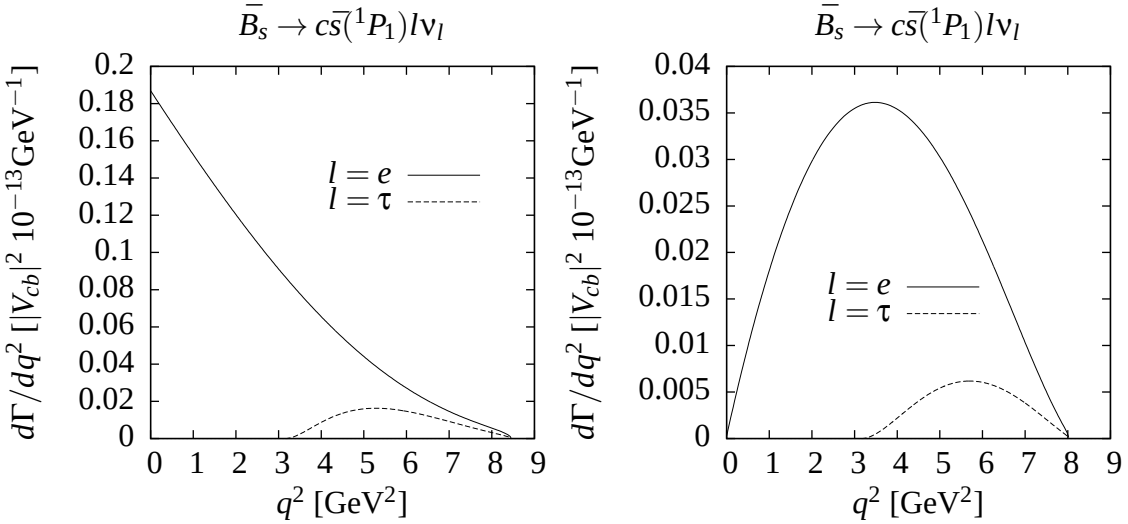

FIG. 7. Differential decay widths for the semileptonic decays of $\bar{B_s}$ into $J^P = 1^+, S = 0$ (left panel) and $J^P = 1^+, S = 1$ (right panel) states.

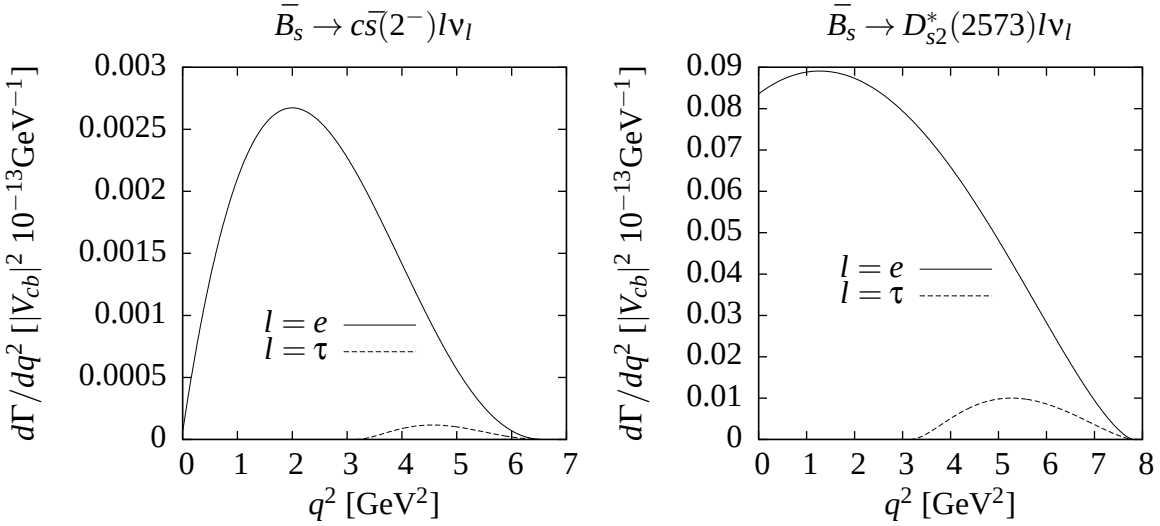

FIG. 8. Differential decay widths for the semileptonic decays of $\bar{B_s}$ into $J^P = 2^-$ (left panel) and $J^P = 2^+$ (right panel) states.

where $r = m_{c\bar{s}}/m_{\bar{B_s}}$. These ratios are expected to vary smoothly with ω.

In the case of the semileptonic decays of B mesons, one expects discrepancies of the order of $10-15\%$ from the predictions of HQET at most. For B_s mesons, one should expect, in principle the same kind of unaccuracies than in the B case. Figure 9 shows that this is indeed the case.

At most, h_- or h_{a_2} differ from 0 at the level of the 15% approximatelly. On the other hand the ratio R_1 gives an estimate of the discrepancies from the Isgur-Wise function, being these much smaller. These negligible corrections to the heavy quark limit

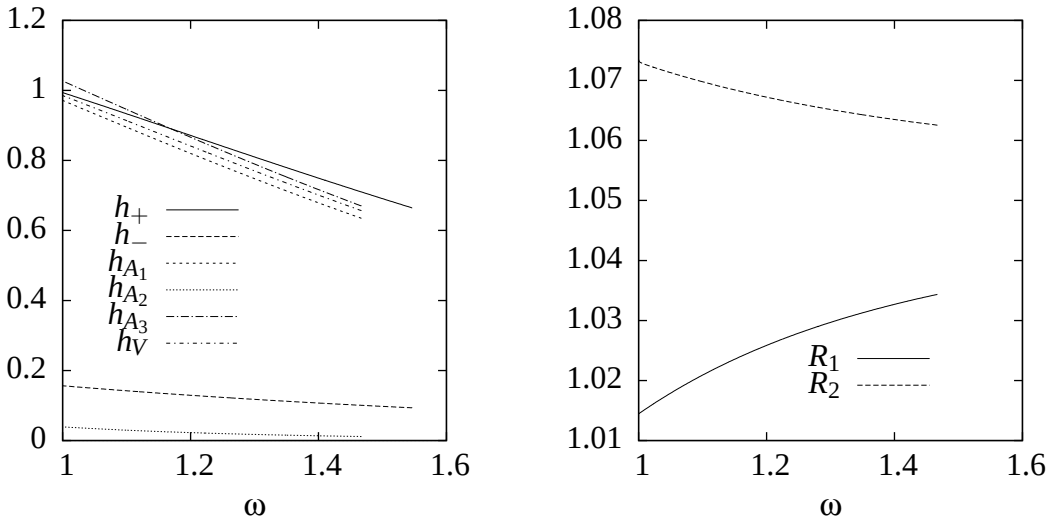

FIG. 9. h form factors for the decay of $\bar{B_s}$ mesons into pseudoscalar and vector $c\bar{s}$ states (left panel) and ratios R_1 and R_2 (right panel).

predictions in the case of h_+ at $\omega = 1$ were also found in the similar calculation carried out in Ref. [23] for the semileptonic $B \to D$ decay, and this quite small violations might be related to the NRCQM approach. Sum rule and lattice calculation predicts somehow larger corrections, though much smaller than those that affect to h_-. This is because Luke's theorem, that guaranties that corrections to $h_+(1)$ are order $O(1/M_Q^2)$.

IV. SEMILEPTONIC $\bar{B_s}$ TO B^- AND B^{*-} DECAYS

In principle, one could also consider those weak processes of B_s driven by the $\bar{s} \to \bar{u}$ decays at the quark level. In this case, due to the similar value of the masses of the $\bar{B_s}$, B and B^* mesons ($m_{\bar{B_s}} - m_{B^-} = 87$ MeV, $m_{\bar{B_s}} - m_{B^{*-}} = 41$ MeV), the only decay modes allowed are the semileptonic $\bar{B_s} \to B^- e^+ \nu_e$ and $\bar{B_s} \to B^{*-} e^+ \nu_e$, as the muon, for instance, lay beyond the scope of the available phase space, so that other semileptonic or nonleptonic processes are forbidden.

Let us consider first the $\bar{B_s} \to B^-$ transition. This process involve a pseudoscalar to pseudoscalar transition, so we take the following form factor decomposition

$$\left\langle B^- \vec{P}_{B^-} \left| J_\mu^{su}(0) \right| \bar{B_s}, \vec{P}_{\bar{B_s}} \right\rangle = P_\mu F_+(q^2) + q_\mu F_-(q^2). \tag{49}$$

The expressions of the form factors are exactly the same of those of Eq. 12.

The total decay width of this process results to be

$$\Gamma_{B_s \to B^- e^+ \nu_e} = 1.7\ 10^{-20}\ \text{GeV} \tag{50}$$

For the process $\bar{B_s} \to B^{*-} e^+ \nu_e$ process. Again, the form factor decomposition is the same as that of the $B_s \to D_s^*$ decay,

$$\begin{aligned}\left\langle B^* \lambda \vec{P}_{c\bar{s}} \left| J_\mu^{su}(0) \right| B_s, \vec{P}_{B_s} \right\rangle = & \frac{-1}{m_{B_s} + m_{c\bar{s}}} \varepsilon_{\mu\nu\alpha\beta} \varepsilon^{\nu *}_{(\lambda)}(\vec{P}_{c\bar{s}}) P^\alpha q^\beta V(q^2) \\ & - i \left\{ (m_{B_s} - m_{c\bar{s}}) \varepsilon^*_{(\lambda)\mu}(\vec{P}_{c\bar{s}}) A_0(q^2) - \frac{P \cdot \varepsilon^*_{(\lambda)}(\vec{P}_{c\bar{s}})}{m_{B_s} + m_{c\bar{s}}} (P_\mu A_+(q^2) + q_\mu A_-(q^2)) \right\},\end{aligned} \tag{51}$$

and the expression of the form factor is that of Eq. 16. Now we obtain

$$\Gamma_{B_s \to B^* e^- \bar{\nu}_e} = 7.6\ 10^{-22}\ \text{GeV} \tag{52}$$

The decay widths of these transitions are several orders of magnitude smaller than other corresponding to reactions involving a $b \to c$ transition. One could expect this fact due to the reduced phase space available for reactions driven by a $s \to u$ transition at the quark level.

V. NONLEPTONIC $B_s \to c\bar{s}M_F$ TWO MESON DECAYS

In this section we evaluate decay widths for nonleptonic $\bar{B_s} \to c\bar{s}M_F$ two-meson decays where M_F is a pseudoscalar or vector meson. These decays correspond to a $b \to c$ transition at the quark level. These transitions are governed, neglecting penguin operators, by the effective Hamiltonian [46, 47]

$$H_{\rm eff} = \frac{G_F}{\sqrt{2}} \left(V_{cb} \left[c_1(\mu) Q_1^{cb} + c_2(\mu) Q_2^{cb} \right] + H.c. \right), \tag{53}$$

where $c_{1,2}$ are scale-dependent Wilson coefficients, and $Q_{1,2}$ are local four-quark operators given by

$$\begin{aligned} Q_1^{cb} =& \bar{\Psi}_c(0)\gamma_\mu(I-\gamma_5)\Psi_b(0) \left[V_{ud}^* \bar{\Psi}_d(0)\gamma^\mu(I-\gamma_5)\Psi_u(0) + V_{us}^* \bar{\Psi}_s(0)\gamma^\mu(I-\gamma_5)\Psi_u(0) \right. \\ & \left. + V_{cd}^* \bar{\Psi}_d(0)\gamma^\mu(I-\gamma_5)\Psi_c(0) + V_{cs}^* \bar{\Psi}_s(0)\gamma^\mu(I-\gamma_5)\Psi_c(0) \right] \\ Q_2^{cb} =& \bar{\Psi}_d(0)\gamma_\mu(I-\gamma_5)\Psi_b(0) \left[V_{ud}^* \bar{\Psi}_c(0)\gamma^\mu(I-\gamma_5)\Psi_u(0) + V_{cd}^* \bar{\Psi}_c(0)\gamma^\mu(I-\gamma_5)\Psi_c(0) \right] \\ & + \bar{\Psi}_s(0)\gamma_\mu(I-\gamma_5)\Psi_b(0) \left[V_{us}^* \bar{\Psi}_c(0)\gamma^\mu(I-\gamma_5)\Psi_u(0) + V_{cs}^* \bar{\Psi}_c(0)\gamma^\mu(I-\gamma_5)\Psi_c(0) \right], \end{aligned} \tag{54}$$

where V_{ij} are CKM matrix elements. We shall work in the factorization approximation, i. e., the hadron matrix elements of the effective Hamiltonian are evaluated as a product of quark-current matrix elements. One of these is the matrix element of the B_s transition to one of the final mesons, while the other corresponds to the transition to the vacuum to the other final mesons, which is given by the corresponding meson decay constant. This is depicted in Fig. 10.

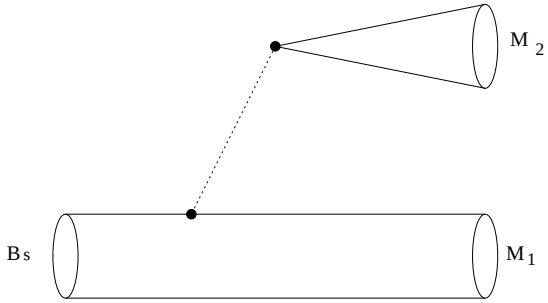

FIG. 10. Diagrammatic representation of $\bar{B_s}$ two meson decay in the factorization approximation.

When writing the factorization amplitude one has to take into account the Fierz reordered contribution so that the relevant coefficients are not c_1 and c_2, but the combinations

$$\begin{aligned} a_1(\mu) &= c_1(\mu) + \frac{1}{N_C} c_2(\mu) \\ a_2(\mu) &= c_2(\mu) + \frac{1}{N_C} c_1(\mu) \end{aligned} \tag{55}$$

with $N_C = 3$ the number of colors. The appropriate energy scale (μ) in our case is $\mu \approx m_b$, providing the following values for $a_{1,2}$ [48]:

$$a_1 = 1.14 \qquad a_2 = -0.20. \tag{56}$$

A. $M_F = \pi, \rho, K, K^*$

For final states containing one of these mesons, the decay width is given by

$$\Gamma = \frac{G_F^2}{16\pi m_{B_s}^2} |V_{bc}|^2 |V_F|^2 \frac{\lambda^{1/2}(m_{B_s}^2, m_{c\bar{s}}^2, m_{M_F})^2}{2m_{B_s}} a_1^2 \mathcal{H}_{\alpha\beta}(P_{B_s}, P_{c\bar{s}}) \hat{\mathcal{H}}^{\alpha\beta}(P_F), \tag{57}$$

	Γ [10^{-15} GeV]		Γ [10^{-15} GeV]		Γ [10^{-15} GeV]
$\bar{B_s} \to D_s^+ \pi^-$	$1.84^{+0.04}_{-0.03}\, a_1^2$	$\bar{B_s} \to D_s^{*+} \pi^-$	$1.56^{+0.1}_{-0.04}\, a_1^2$	$\bar{B_s} \to (2^-)^+ \pi^-$	$2.46^{+0.09}_{-0.27}\, 10^{-4}\, a_1^2$
$\bar{B_s} \to D_s^+ \rho^-$	$4.53^{+0.1}_{-0.09}\, a_1^2$	$\bar{B_s} \to D_s^{*+} \rho^-$	$4.67^{+0.3}_{-0.11}\, a_1^2$	$\bar{B_s} \to (2^-)^+ \rho^-$	$1.62_{-0.26}\, 10^{-2}\, a_1^2$
$\bar{B_s} \to D_s^+ K^-$	$0.14^{+0.01}\, a_1^2$	$\bar{B_s} \to D_s^{*+} K^-$	$0.12^{+0.01}_{-0.01}\, a_1^2$	$\bar{B_s} \to (2^-)^+ K^-$	$1.82^{+0.06}_{-0.2}\, 10^{-5}\, a_1^2$
$\bar{B_s} \to D_s^+ K^{*-}$	$0.25^{0.01}_{-0.01}\, a_1^2$	$\bar{B_s} \to D_s^{*+} K^{*-}$	$0.27^{+0.02}_{-0.01}\, a_1^2$	$\bar{B_s} \to (2^-)^+ K^{*-}$	$1.11_{-0.12}\, 10^{-3}\, a_1^2$
$\bar{B_s} \to D_{s0}^{*+} \pi^-$	$0.39^{+0.01}_{-0.01}\, a_1^2$	$\bar{B_s} \to D_{s1}^+(2460) \pi^-$	$0.53_{-0.02}\, a_1^2$	$\bar{B_s} \to D_{s2}^{*+} \pi^-$	$0.35_{-0.03}\, a_1^2$
$\bar{B_s} \to D_{s0}^{*+} \rho^-$	$0.94^{+0.04}_{-0.04}\, a_1^2$	$\bar{B_s} \to D_{s1}^+(2460) \rho^-$	$1.26_{-0.06}\, a_1^2$	$\bar{B_s} \to D_{s2}^{*+} \rho^-$	$0.95_{-0.07}\, a_1^2$
$\bar{B_s} \to D_{s0}^{*+} K^-$	$2.98^{+0.11}_{-0.15}\, 10^{-2}\, a_1^2$	$\bar{B_s} \to D_{s1}^+(2460) K^-$	$4.09_{-0.1}\, 10^{-2}\, a_1^2$	$\bar{B_s} \to D_{s2}^{*+} K^-$	$2.61_{-0.17}\, 10^{-2}\, a_1^2$
$\bar{B_s} \to D_{s0}^{*+} K^{*-}$	$5.19^{+0.18}_{-0.24}\, 10^{-2}\, a_1^2$	$\bar{B_s} \to D_{s1}^+(2460) K^{*-}$	$6.93_{-0.3}\, 10^{-2}\, a_1^2$	$\bar{B_s} \to D_{s2}^{*+} K^{*-}$	$5.41_{-0.37}\, 10^{-2}\, a_1^2$
		$\bar{B_s} \to D_{s1}^+(2536) \pi^-$	$0.25_{-0.01}\, a_1^2$		
		$\bar{B_s} \to D_{s1}^+(2536) \rho^-$	$0.66_{-0.03}\, a_1^2$		
		$\bar{B_s} \to D_{s1}^+(2536) K^-$	$1.94_{-0.08}\, 10^{-2}\, a_1^2$		
		$\bar{B_s} \to D_{s1}^+(2536) K^{*-}$	$3.75_{-0.2}\, 10^{-2}\, a_1^2$		

TABLE VIII. Total nonleptonic decay widths of B_s mesons for generic values of the Wilson parameter a_1. The central values have been calculated using the AL1 potential.

where m_f is the mass of the M_F meson, V_F is V_{ud} for $M_F = \pi, \rho$ and V_{us} for $M_F = K, K^*$. $\mathcal{H}_{\alpha\beta}(P_{B_s}, P_{c\bar{s}})$ is the hadron tensor accounting for the $B_s \to c\bar{s}$ transition, while the other, $\mathcal{H}^{\alpha\beta}(P_F)$ corresponds to a vacuum $\to M_F$ transition. This is equal to

$$\hat{\mathcal{H}}^{\alpha\beta}(P_F) = p_F^\alpha p_F^\beta f_F^2 \tag{58}$$

for a pseudoscalar M_F, and

$$\hat{\mathcal{H}}^{\alpha\beta}(P_F) = (p_F^\alpha p_F^\beta - m_F^2 g^{\alpha\beta}) f_F^2 \tag{59}$$

for a vector M_F. All the necessary meson decay constants can be found in Table II.

As we did in the case of semileptonic decays, the contraction of the two hadron tensors can be written in terms of helicity amplitudes. For a pseudoscalar M_F, this is

$$\mathcal{H}_{\alpha\beta} \tilde{\mathcal{H}}^{\alpha\beta} = \mathcal{H}_{tt}(m_F^2) m_F^2 f_F^2, \tag{60}$$

and for a vector M_F,

$$\mathcal{H}_{\alpha\beta} \tilde{\mathcal{H}}^{\alpha\beta} = m_F^2 f_F^2 \left(\mathcal{H}_{+1+1}(m_F^2) + \mathcal{H}_{-1-1}(m_F^2) + \mathcal{H}_{00}(m_F^2) \right) \tag{61}$$

In Table VIII we show the values for the decay widths we obtain for the nonleptonic decay widths of the different channels considered in units of 10^{-15}GeV. In Table IX we express our results as branching fractions and compare with other calculations. As shown there, our results agree with those from Refs. [28] and [36] in which relativistic CQM and QCD sum rules techniques were used, respectively. Our results for decays with a vector D_s^* in the final state also agree finely with those from [32], although our values for final states with a pseudoscalar D_s meson in the final state are about a factor 2 larger than those from [32], who also works in the context of nonrelativistic constituent quark models. The values calculated in this work are larger by a factor 2 or more than the results from Refs. [33], [49] and [50], in which a light cone sum rules, QCD sum rules and covariant light front quark model approaches have been used. Finally we compare our results with the experimental measurements enclosed in Ref. [39].

B. $M_F = D, D_s, D^*, D_s^*$

In the same way, we can calculate the nonleptonic decay width of the processes $\bar{B_s} \to D_s D$, $\bar{B_s} \to D_s D^*$, $\bar{B_s} \to D_s^* D_s$, $\bar{B_s} \to D_s^* D_s^*$, $\bar{B_s} \to D_s D_s^*$, and $\bar{B_s} \to D_s^* D_s^*$ decays. As in the previous case, there is only one contribution proportional to the coefficient a_1, with momentum transfer ranges between m_D^2 and $m_{D^*}^2$. These momentum transfers are neither too high (so there is no need to involve a B_s^* resonance) nor too low (with a high trimomentum transfer). For $M_F = D, D^*, D_S, D_s^*$, the relevant contractions for the hadron tensors can be obtained from Eqs. 60 and 61, performing straigthforward substitutions. As in the previous case, the decay constants relevant for these calculations can be found in Table II.

	This work	[28]	[36]	[32]	[33]	[49]	[50]	Experiment [39]
$\bar{B_s} \to D_s^+ \pi^-$	0.53	0.35	0.5	$0.27^{+0.07}_{-0.03}$	$0.17^{+0.07}_{-0.06}$	0.142 ± 0.57	$0.196^{+0.123}_{-0.097}$	0.32 ± 0.4
$\bar{B_s} \to D_s^+ \rho^-$	1.26	0.94	1.3	$0.64^{+0.17}_{-0.11}$	$0.42^{+1.7}_{-1.4}$		$0.47^{+2.9}_{-2.3}$	0.74 ± 0.17
$\bar{B_s} \to D_s^+ K^-$	0.04	0.028	0.04	$0.021^{+0.002}_{-0.002}$	$0.013^{+0.005}_{-0.004}$	0.0103 ± 0.0051	$0.017^{+0.0087}_{-0.0066}$	
$\bar{B_s} \to D_s^+ K^{*-}$	0.08	0.047	0.06	$0.038^{+0.005}_{-0.005}$	$0.028^{+0.01}_{-0.08}$	0.005 ± 0.0022		
$\bar{B_s} \to D_{s0}^{*+} \pi^-$	0.10	0.09	$0.052^{+0.25}_{-0.021}$					
$\bar{B_s} \to D_{s0}^{*+} \rho^-$	0.27	0.22	$0.013^{+0.06}_{-0.05}$					
$\bar{B_s} \to D_{s0}^{*+} K^-$	0.009	0.007	$0.004^{+0.002}_{-0.002}$					
$\bar{B_s} \to D_{s0}^{*+} K^{*-}$	0.16	0.012	$0.008^{+0.004}_{-0.003}$					
$\bar{B_s} \to D_s^{*+} \pi^-$	0.45	0.27	0.2	$0.31^{+0.03}_{-0.02}$		0.211 ± 0.073	$0.189^{+0.120}_{-0.093}$	0.21 ± 0.06
$\bar{B_s} \to D_s^{*+} \rho^-$	1.35	0.87	1.3	$0.9^{+1.5}_{-1.5}$			$0.523^{+0.334}_{-0.256}$	1.03 ± 2.6
$\bar{B_s} \to D_s^{*+} K^-$	0.04	0.021	0.02	$0.024^{+0.002}_{-0.002}$				
$\bar{B_s} \to D_s^{*+} K^{*-}$	0.08	0.048	0.06	$0.056^{+0.006}_{-0.007}$				
$\bar{B_s} \to D_{s1}^{+}(2460) \pi^-$	0.15	0.19						
$\bar{B_s} \to D_{s1}^{+}(2460) \rho^-$	0.36	0.49						
$\bar{B_s} \to D_{s1}^{+}(2460) K^-$	0.012	0.014						
$\bar{B_s} \to D_{s1}^{+}(2460) K^{*-}$	0.020	0.026						
$\bar{B_s} \to D_{s1}^{+}(2536) \pi^-$	0.07	0.029						
$\bar{B_s} \to D_{s1}^{+}(2536) \rho^-$	0.19	0.083						
$\bar{B_s} \to D_{s1}^{+}(2536) K^-$	0.0054	0.0021						
$\bar{B_s} \to D_{s1}^{+}(2536) K^{*-}$	0.01	0.0044						
$\bar{B_s} \to (2^-)^+ \pi^-$	$7.1\ 10^{-5}$							
$\bar{B_s} \to (2^-)^+ \rho^-$	0.0047							
$\bar{B_s} \to (2^-)^+ K^-$	$5.2\ 10^{-6}$							
$\bar{B_s} \to (2^-)^+ K^{*-}$	$2.2\ 10^{-8}$							
$\bar{B_s} \to D_{s2}^{*+} \pi^-$	0.1	0.16						
$\bar{B_s} \to D_{s2}^{*+} \rho^-$	0.27	0.42						
$\bar{B_s} \to D_{s2}^{*+} K^-$	0.008	0.012						
$\bar{B_s} \to D_{s2}^{*+} K^{*-}$	0.016	0.022						

TABLE IX. Branching ratios for the decays above.

	$\Gamma\ [10^{-15}\ \text{GeV}]$
$\bar{B_s} \to D_s^+ D_s^-$	$7.35^{+0.04}_{-0.14}\, a_1^2$
$\bar{B_s} \to D_s^+ D_s^{*-}$	$6.89^{+0.02}_{-0.13}\, a_1^2$
$\bar{B_s} \to D_s^{*+} D_s^-$	$4.23_{-0.38}\, a_1^2$
$\bar{B_s} \to D_s^{*+} D_s^{*-}$	$18.79_{-1.6}\, a_1^2$
$\bar{B_s} \to D_s^+ D^-$	$0.25_{-0.01}\, a_1^2$
$\bar{B_s} \to D_s^+ D^{*-}$	$0.19_{-0.01}\, a_1^2$
$\bar{B_s} \to D_s^{*+} D^-$	$0.15^{+0.01}_{-0.01}\, a_1^2$
$\bar{B_s} \to D_s^{*+} D^{*-}$	$0.46^{+0.02}_{-0.01}\, a_1^2$

TABLE X. Nonleptonic decay widths for the indicated processes indicated, using the factorization approximation. We give our results for generic values of the parameter a_1.

Results are enclosed in Table X. In Table XI, we present our values as branching fractions, and compare with other results, in the case of decays with two $D_s^{(*)}$ mesons in the final state. We have found a fair agreement with the branching fractions calculated in [28] and [36], and larger differences with the values given in [32], [33] and [51]. Most of the values calculated here and those found in the literature differ from the experimental results by a factor around 2. Appart from the inaccuracies of the factorization approximation, the results are sensitive, not only two the Wilson parameter a_1, also on the value that have been used for the mesons decay constant and on the overlap among the wave functions used to calculate the matrix elements.

	This work	[28]	[36]	[32]	[33]	[51]	Experiment [39]
$\bar{B_s} \to D_s^+ D_s^-$	2.1	1.1	1.0	$0.83^{+0.1}_{-0.1}$	1.65	0.217 ± 0.082	0.53 ± 0.09
$\bar{B_s} \to D_s^+ D_s^{*-}$	2.0	1.0	0.8	$0.84^{+0.12}_{-0.12}$		0.262 ± 0.93	
$\bar{B_s} \to D_s^{*+} D_s^-$	1.24	0.61	0.4	$0.7^{+1.6}_{-0.15}$		0.254 ± 0.57	
$\bar{B_s} \to D_s^+ D_s^{*-} + D_s^{*+} D_s^-$	3.24	1.61	1.2	$1.54^{+0.2}_{-0.19}$	2.4	5.16 ± 0.11	1.24 ± 0.21
$\bar{B_s} \to D_s^{*+} D_s^{*-}$	5.45	2.5	1.6	$2.4^{+0.4}_{-0.4}$	3.18	2.77 ± 0.76	1.88 ± 0.34
$\bar{B_s} \to D_s^{(*)+} D_s^{(*)-}$	10.8	5.21	3.8	$4.77^{+0.46}_{-0.46}$	7.23	3.5 ± 0.78	4.5 ± 1.4
$\bar{B_s} \to D_s^+ D^-$	0.08						
$\bar{B_s} \to D_s^+ D^{*-}$	0.05						
$\bar{B_s} \to D_s^{*+} D^-$	0.04						
$\bar{B_s} \to D_s^{*+} D^{*-}$	0.13						

TABLE XI. Branching ratios in % for the decays indicated above. We also compare with other calculations.

	Γ [10^{-15} GeV]	BR in %	Experiment [39]
$\bar{B_s} \to \phi J/\Psi$	$11.80^{+1.9}_{-0.8}\, a_2^2$	0.11	$(0.109^{+0.28}_{-0.23})$
$\bar{B_s} \to K^0 J/\Psi$	$8.1^{+0.5}_{-1.3}\, 10^{-2}\, a_2^2$	$7.25\ 10^{-4}$	$(3.6 \pm 0.8)\ 10^{-3}$
$\bar{B_s} \to K^{*0} J/\Psi$	$0.51_{-0.3}\, a_2^2$	$4.6\ 10^{-3}$	$(9 \pm 4)\ 10^{-3}$

TABLE XII. Branching ratios in % for the reactions indicated above. We give our results for generic values of a_2.

VI. OTHER NONLEPTONIC DECAYS

The calculation of decay channels

$$\begin{aligned} \bar{B_s} &\to \phi J/\Psi \\ \bar{B_s} &\to K^0 J/\Psi \\ \bar{B_s} &\to K^{*0} J/\Psi \end{aligned} \tag{62}$$

in the factorization approximation can be easily performed. Their decay width are summarized in Table XII.

In Table XII we also give the branching fractions of these channels in %, for generic values of the Wilson parameter a_2, and compare with the experimental measurements. Our result for the branching ratio corresponding to the decay into $K^0 J/\Psi$ states reproduces roughly the order of magnitude of the corresponding experimental value ($\approx 10^{-3}$). In contrast, our results for the branching fractions for the $\bar{B_s} \to \phi J/\Psi$ and $\bar{B_s} \to K^{*0} J/\Psi$ decays agree with the experimental data of Ref. [39].

VII. SUMMARY AND CONCLUSIONS

In this paper we have studied the semileptonic decays of the $\bar{B_s}$ meson into $c\bar{s}$ states with $J^P = 0^-, 0^+, 1^-, 1^+, 2^-$ and 2^+. We have worked in the context of nonrelativistic constituent quark models. We compare with the experimental results enclosed in Ref. [39] when possible. We have also computed several nonleptonic decay modes of $\bar{B_s}$ mesons. We work in the factorization approximation, as the momenta involved does not involve resonances or high trimomentum transfer. We give results for general values of the Wilson coefficients. We give an estimate of our theoretical uncertainties by considering different sets of wave functions derived from the quark–antiquark potentials of Ref. [42]. The results that we obtain for the semileptonic decay width are in general in good agreement with previous calculations and with the available experimental measurements. In the case of the nonleptonic decay channels that we have studied, we have found reasonable agreement with previous calculations. The nonleptonic decays of $\bar{B_s}$ mesons into $\phi J/\Psi$, $K^0 J/\Psi$ and $K^{*0}(892) J/\Psi$ have been considered in this work, finding a good agreement with the experimental results.

ACKNOWLEDGMENTS

The author thanks J. Nieves, E. Hernández, M. Á. Pérez-García, I. Vidaña and S. Chiacchiera for useful discussions and kind hospitality. The author also thanks the Physics Department at the University of Coimbra and Departamento de Física Fundamental at University of Salamanca for their hospitality. The author acknowledges a contract from the CPAN project and support from Junta de Andaluca under contract FQM-225.

Appendix A: Expressions for the matrix elements

- Case $J^\pi = 0^-$

$$V^0(|\vec{q}|) = \sqrt{2m_I 2E_F(-\vec{q})} \int d^3p \, \frac{1}{4\pi} \left(\hat{\phi}^{(M_F(0^-))}_{f_1', f_2}(|\vec{p}|)\right)^* \hat{\phi}^{(M_I(0^-))}_{f_1, f_2} \left(\left|\vec{p} - \frac{m_{f_2}}{m_{f_1'} + m_{f_2}}|\vec{q}|\vec{k}\right|\right) \sqrt{\frac{\widehat{E}_{f_1'}\widehat{E}_{f1}}{4E_{f_1'}E_{f_1}}} \left(1 + \frac{(-\frac{m_{f_1'}}{m_{f_1'}+m_{f_2}}|\vec{q}|\vec{k} - \vec{p}) \cdot (\frac{m_{f_2}}{m_{f_1'}+m_{f_2}}|\vec{q}|\vec{k} - \vec{p})}{\widehat{E}_{f_1'}\widehat{E}_{f_1}}\right)$$

$$V^3(|\vec{q}|) = \sqrt{2m_I 2E_F(-\vec{q})} \int d^3p \, \frac{1}{4\pi} \left(\hat{\phi}^{(M_F(0^-))}_{f_1', f_2}(|\vec{p}|)\right)^* \hat{\phi}^{(M_I(0^-))}_{f_1, f_2} \left(\left|\vec{p} - \frac{m_{f_2}}{m_{f_1'} + m_{f_2}}|\vec{q}|\vec{k}\right|\right) \sqrt{\frac{\widehat{E}_{f_1'}\widehat{E}_{f1}}{4E_{f_1'}E_{f_1}}} \left(\frac{\frac{m_{f_2}}{m_{f_1'}+m_{f_2}}|\vec{q}| - p_z}{\widehat{E}_{f_1}} + \frac{-\frac{m_{f_1'}}{m_{f_1'}+m_{f_2}}|\vec{q}| - p_z}{\widehat{E}_{f_1'}}\right) \tag{A1}$$

- Case $J^\pi = 0^+$

$$A^0(|\vec{q}|) = \sqrt{2m_I 2E_F(-\vec{q})} \int d^3p \, \frac{1}{4\pi|\vec{p}|} \left(\hat{\phi}^{(M_F(0^+))}_{f_1', f_2}(|\vec{p}|)\right)^* \hat{\phi}^{(M_I(0^-))}_{f_1, f_2} \left(\left|\vec{p} - \frac{m_{f_2}}{m_{f_1'} + m_{f_2}}|\vec{q}|\vec{k}\right|\right) \sqrt{\frac{\widehat{E}_{f_1'}\widehat{E}_{f1}}{4E_{f_1'}E_{f_1}}} \left(\frac{\vec{p} \cdot (\frac{m_{f_2}}{m_{f_1'}+m_{f_2}}|\vec{q}|\vec{k} - \vec{p})}{\widehat{E}_{f_1}} + \frac{\vec{p} \cdot (-\frac{m_{f_1'}}{m_{f_1'}+m_{f_2}}|\vec{q}|\vec{k} - \vec{p})}{\widehat{E}_{f_1'}}\right)$$

$$A^3(|\vec{q}|) = \sqrt{2m_I 2E_F(-\vec{q})} \int d^3p \, \frac{1}{4\pi|\vec{p}|} \left(\hat{\phi}^{(M_F(0^+))}_{f_1', f_2}(|\vec{p}|)\right)^* \hat{\phi}^{(M_I(0^-))}_{f_1, f_2} \left(\left|\vec{p} - \frac{m_{f_2}}{m_{f_1'} + m_{f_2}}|\vec{q}|\vec{k}\right|\right) \sqrt{\frac{\widehat{E}_{f_1'}\widehat{E}_{f1}}{4E_{f_1'}E_{f_1}}} \Bigg\{ p_z \left(1 - \frac{(-\frac{m_{f_1'}}{m_{f_1'}+m_{f_2}}|\vec{q}|\vec{k} - \vec{p}) \cdot (\frac{m_{f_2}}{m_{f_1'}+m_{f_2}}|\vec{q}|\vec{k} - \vec{p})}{\widehat{E}_{f_1'}\widehat{E}_{f_1}}\right) + \frac{1}{\widehat{E}_{f_1'}\widehat{E}_{f1}} \Bigg[\left(-\frac{m_{f_1'}}{m_{f_1'}+m_{f_2}}|\vec{q}| - p_z\right) \vec{p} \cdot \left(\frac{m_{f_2}}{m_{f_1'}+m_{f_2}}|\vec{q}|\vec{k} - \vec{p}\right) + \left(\frac{m_{f_2}}{m_{f_1'}+m_{f_2}}|\vec{q}| - p_z\right) \vec{p} \cdot \left(-\frac{m_{f_1'}}{m_{f_1'}+m_{f_2}}|\vec{q}|\vec{k} - \vec{p}\right) \Bigg] \Bigg\} \tag{A2}$$

- Case $J^\pi = 1^-$

$$V^{(1^-)1}_{\lambda=-1}(|\vec{q}|) = \frac{-i}{\sqrt{2}} \sqrt{2m_I 2E_F(-\vec{q})} \int d^3p \, \frac{1}{4\pi} \left(\hat{\phi}^{(M_F(1^-))}_{f_1', f_2}(|\vec{p}|)\right)^* \hat{\phi}^{(M_I(0^-))}_{f_1, f_2} \left(\left|\vec{p} - \frac{m_{f_2}}{m_{f_1'} + m_{f_2}}|\vec{q}|\vec{k}\right|\right) \sqrt{\frac{\widehat{E}_{f_1'}\widehat{E}_{f1}}{4E_{f_1'}E_{f_1}}} \left(-\frac{\frac{m_{f_2}}{m_{f_1'}+m_{f_2}}|\vec{q}| - p_z}{\widehat{E}_{f_1}} + \frac{-\frac{m_{f_1'}}{m_{f_1'}+m_{f_2}}|\vec{q}| - p_z}{\widehat{E}_{f_1'}}\right) \tag{A3}$$

$$
\begin{aligned}
A^{(1^-)\,0}_{\lambda=0}(|\vec{q}|) &= i\,\sqrt{2m_I 2E_F(-\vec{q})}\int d^3p\,\frac{1}{4\pi}\left(\hat{\phi}^{(M_F(1^-))}_{f_1',f_2}(|\vec{p}|)\right)^*\hat{\phi}^{(M_I(0^-))}_{f_1,f_2}\left(\left|\vec{p}-\frac{m_{f_2}}{m_{f_1'}+m_{f_2}}|\vec{q}|\vec{k}\right|\right)\\
&\quad\sqrt{\frac{\widehat{E}_{f_1'}\widehat{E}_{f1}}{4E_{f_1'}E_{f_1}}}\left(\frac{\frac{m_{f_2}}{m_{f_1'}+m_{f_2}}|\vec{q}|-p_z}{\widehat{E}_{f_1}}+\frac{-\frac{m_{f_1'}}{m_{f_1'}+m_{f_2}}|\vec{q}|-p_z}{\widehat{E}_{f_1'}}\right)\\
A^{(1^-)\,1}_{\lambda=-1}(|\vec{q}|) &= \frac{i}{\sqrt{2}}\sqrt{2m_I 2E_F(-\vec{q})}\int d^3p\,\frac{1}{4\pi}\left(\hat{\phi}^{(M_F(1^-))}_{f_1',f_2}(|\vec{p}|)\right)^*\hat{\phi}^{(M_I(0^-))}_{f_1,f_2}\left(\left|\vec{p}-\frac{m_{f_2}}{m_{f_1'}+m_{f_2}}|\vec{q}|\vec{k}\right|\right)\\
&\quad\sqrt{\frac{\widehat{E}_{f_1'}\widehat{E}_{f1}}{4E_{f_1'}E_{f_1}}}\left(1+\frac{2p_x^2-(-\frac{m_{f_1'}}{m_{f_1'}+m_{f_2}}|\vec{q}|\vec{k}-\vec{p})\cdot(\frac{m_{f_2}}{m_{f_1'}+m_{f_2}}|\vec{q}|\vec{k}-\vec{p})}{\widehat{E}_{f_1'}\widehat{E}_{f_1}}\right)\\
A^{(1^-)\,3}_{\lambda=0}(|\vec{q}|) &= i\sqrt{2m_I 2E_F(-\vec{q})}\int d^3p\,\frac{1}{4\pi}\left(\hat{\phi}^{(M_F(1^-))}_{f_1',f_2}(|\vec{p}|)\right)^*\hat{\phi}^{(M_I(0^-))}_{f_1,f_2}\left(\left|\vec{p}-\frac{m_{f_2}}{m_{f_1'}+m_{f_2}}|\vec{q}|\vec{k}\right|\right)\\
&\quad\sqrt{\frac{\widehat{E}_{f_1'}\widehat{E}_{f1}}{4E_{f_1'}E_{f_1}}}\left(1+\frac{2(-\frac{m_{f_1'}}{m_{f_1'}+m_{f_2}}|\vec{q}|-p_z)\cdot(\frac{m_{f_2}}{m_{f_1'}+m_{f_2}}|\vec{q}|-p_z)}{\widehat{E}_{f_1'}\widehat{E}_{f_1}}\right.\\
&\quad\left.-\frac{(-\frac{m_{f_1'}}{m_{f_1'}+m_{f_2}}|\vec{q}|\vec{k}-\vec{p})\cdot(\frac{m_{f_2}}{m_{f_1'}+m_{f_2}}|\vec{q}|\vec{k}-\vec{p})}{\widehat{E}_{f_1'}\widehat{E}_{f_1}}\right)
\end{aligned}
\tag{A4}
$$

- Case $J^\pi = 1^+$

$$
\begin{aligned}
V^{(1^+,S_{q\bar{q}}=0)\,0}_{\lambda=0}(|\vec{q}|) &= i\sqrt{3}\sqrt{2m_I 2E_F(-\vec{q})}\int d^3p\,\frac{1}{4\pi|\vec{p}|}\left(\hat{\phi}^{(M_F(1^+,S_{q\bar{q}}=0))}_{f_1',f_2}(|\vec{p}|)\right)^*\hat{\phi}^{(M_I(0^-))}_{f_1,f_2}\left(\left|\vec{p}-\frac{m_{f_2}}{m_{f_1'}+m_{f_2}}|\vec{q}|\vec{k}\right|\right)\\
&\quad\sqrt{\frac{\widehat{E}_{f_1'}\widehat{E}_{f1}}{4E_{f_1'}E_{f_1}}}\,p_z\left(1+\frac{(-\frac{m_{f_1'}}{m_{f_1'}+m_{f_2}}|\vec{q}|\vec{k}-\vec{p})\cdot(\frac{m_{f_2}}{m_{f_1'}+m_{f_2}}|\vec{q}|\vec{k}-\vec{p})}{\widehat{E}_{f_1'}\widehat{E}_{f_1}}\right)\\
V^{(1^+,S_{q\bar{q}}=1)\,0}_{\lambda=0}(|\vec{q}|) &= -i\sqrt{\frac{3}{2}}\sqrt{2m_I 2E_F(-\vec{q})}\int d^3p\,\frac{1}{4\pi|\vec{p}|}\left(\hat{\phi}^{(M_F(1^+,S_{q\bar{q}}=1))}_{f_1',f_2}(|\vec{p}|)\right)^*\hat{\phi}^{(M_I(0^-))}_{f_1,f_2}\left(\left|\vec{p}-\frac{m_{f_2}}{m_{f_1'}+m_{f_2}}|\vec{q}|\vec{k}\right|\right)\\
&\quad\sqrt{\frac{\widehat{E}_{f_1'}\widehat{E}_{f1}}{4E_{f_1'}E_{f_1}}}\,\frac{|\vec{q}|(p_z^2-\vec{p}^2)}{\widehat{E}_{f_1'}\widehat{E}_{f1}}\\
V^{(1^+,S_{q\bar{q}}=0)\,1}_{\lambda=-1}(|\vec{q}|) &= -i\sqrt{\frac{3}{2}}\sqrt{2m_I 2E_F(-\vec{q})}\int d^3p\,\frac{1}{4\pi|\vec{p}|}\left(\hat{\phi}^{(M_F(1^+,S_{q\bar{q}}=0))}_{f_1',f_2}(|\vec{p}|)\right)^*\hat{\phi}^{(M_I(0^-))}_{f_1,f_2}\left(\left|\vec{p}-\frac{m_{f_2}}{m_{f_1'}+m_{f_2}}|\vec{q}|\vec{k}\right|\right)\\
&\quad\sqrt{\frac{\widehat{E}_{f_1'}\widehat{E}_{f1}}{4E_{f_1'}E_{f_1}}}\,p_x^2\left(\frac{1}{\widehat{E}_{f_1}}+\frac{1}{\widehat{E}_{f_1'}}\right)\\
V^{(1^+,S_{q\bar{q}}=1)\,1}_{\lambda=-1}(|\vec{q}|) &= i\frac{\sqrt{3}}{2}\sqrt{2m_I 2E_F(-\vec{q})}\int d^3p\,\frac{1}{4\pi|\vec{p}|}\left(\hat{\phi}^{(M_F(1^+,S_{q\bar{q}}=1))}_{f_1',f_2}(|\vec{p}|)\right)^*\hat{\phi}^{(M_I(0^-))}_{f_1,f_2}\left(\left|\vec{p}-\frac{m_{f_2}}{m_{f_1'}+m_{f_2}}|\vec{q}|\vec{k}\right|\right)\\
&\quad\sqrt{\frac{\widehat{E}_{f_1'}\widehat{E}_{f1}}{4E_{f_1'}E_{f_1}}}\left(\frac{p_y^2+p_z^2+p_z|\vec{q}|\frac{m_{f_1'}}{m_{f_1'}+m_{f_2}}}{\widehat{E}_{f_1'}}-\frac{p_y^2+p_z^2-p_z|\vec{q}|\frac{m_{f_2}}{m_{f_1'}+m_{f_2}}}{\widehat{E}_{f_1}}\right)
\end{aligned}
$$

$$V_{\lambda=0}^{(1^+,S_{q\bar{q}}=0)3}(|\vec{q}|) = i\sqrt{3}\sqrt{2m_I 2E_F(-\vec{q})}\int d^3p\,\frac{1}{4\pi|\vec{p}|}\left(\hat{\phi}^{(M_F(1^+,S_{q\bar{q}}=0))}_{f_1',f_2}(|\vec{p}|)\right)^*\hat{\phi}^{(M_I(0^-))}_{f_1,f_2}\left(\left|\vec{p}-\frac{m_{f_2}}{m_{f_1'}+m_{f_2}}|\vec{q}|\vec{k}\right|\right)$$
$$\sqrt{\frac{\widehat{E}_{f_1'}\widehat{E}_{f1}}{4E_{f_1'}E_{f_1}}}\,p_z\left(\frac{\frac{m_{f_2}}{m_{f_1'}+m_{f_2}}|\vec{q}|-p_z}{\widehat{E}_{f_1}}+\frac{-\frac{m_{f_1'}}{m_{f_1'}+m_{f_2}}|\vec{q}|-p_z}{\widehat{E}_{f_1'}}\right)$$

$$V_{\lambda=0}^{(1^+,S_{q\bar{q}}=1)3}(|\vec{q}|) = -i\sqrt{\frac{3}{2}}\sqrt{2m_I 2E_F(-\vec{q})}\int d^3p\,\frac{1}{4\pi|\vec{p}|}\left(\hat{\phi}^{(M_F(1^+,S_{q\bar{q}}=1))}_{f_1',f_2}(|\vec{p}|)\right)^*\hat{\phi}^{(M_I(0^-))}_{f_1,f_2}\left(\left|\vec{p}-\frac{m_{f_2}}{m_{f_1'}+m_{f_2}}|\vec{q}|\vec{k}\right|\right)$$
$$\sqrt{\frac{\widehat{E}_{f_1'}\widehat{E}_{f1}}{4E_{f_1'}E_{f_1}}}\,(p_x^2+p_y^2)\left(\frac{1}{\widehat{E}_{f_1}}-\frac{1}{\widehat{E}_{f_1'}}\right)$$

$$A_{\lambda=-1}^{(1^+,S_{q\bar{q}}=0)1}(|\vec{q}|) = -i\sqrt{\frac{3}{2}}\sqrt{2m_I 2E_F(-\vec{q})}\int d^3p\,\frac{1}{4\pi|\vec{p}|}\left(\hat{\phi}^{(M_F(1^+,S_{q\bar{q}}=0))}_{f_1',f_2}(|\vec{p}|)\right)^*\hat{\phi}^{(M_I(0^-))}_{f_1,f_2}\left(\left|\vec{p}-\frac{m_{f_2}}{m_{f_1'}+m_{f_2}}|\vec{q}|\vec{k}\right|\right)$$
$$\sqrt{\frac{\widehat{E}_{f_1'}\widehat{E}_{f1}}{4E_{f_1'}E_{f_1}}}\,\frac{p_y^2|\vec{q}|}{\widehat{E}_{f_1}\widehat{E}_{f_1'}}$$

$$A_{\lambda=-1}^{(1^+,S_{q\bar{q}}=1)1}(|\vec{q}|) = i\frac{\sqrt{3}}{2}\sqrt{2m_I 2E_F(-\vec{q})}\int d^3p\,\frac{1}{4\pi|\vec{p}|}\left(\hat{\phi}^{(M_F(1^+,S_{q\bar{q}}=1))}_{f_1',f_2}(|\vec{p}|)\right)^*\hat{\phi}^{(M_I(0^-))}_{f_1,f_2}\left(\left|\vec{p}-\frac{m_{f_2}}{m_{f_1'}+m_{f_2}}|\vec{q}|\vec{k}\right|\right)$$
$$\sqrt{\frac{\widehat{E}_{f_1'}\widehat{E}_{f1}}{4E_{f_1'}E_{f_1}}}\left\{\,p_z\left(1-\frac{(-\frac{m_{f_1'}}{m_{f_1'}+m_{f_2}}|\vec{q}|\vec{k}-\vec{p})\cdot(\frac{m_{f_2}}{m_{f_1'}+m_{f_2}}|\vec{q}|\vec{k}-\vec{p})}{\widehat{E}_{f_1'}\widehat{E}_{f_1}}\right)\right.$$
$$\left.+\frac{m_{f_2}-m_{f_1'}}{m_{f_1'}+m_{f_2}}\frac{p_x^2|\vec{q}|}{\widehat{E}_{f_1'}\widehat{E}_{f1}}\right\}$$

(A5)

- Case $J^\pi = 2^-$

$$V_{T\lambda=0}^{(2^-)0}(|\vec{q}|) = i\sqrt{\frac{15}{2}}\sqrt{2m_I 2E_F(-\vec{q})}\int d^3p\,\frac{1}{4\pi|\vec{p}|^2}\left(\hat{\phi}^{(M_F(2^-))}_{f_1',f_2}(|\vec{p}|)\right)^*\hat{\phi}^{(M_I(0^-))}_{f_1,f_2}\left(\left|\vec{p}-\frac{m_{f_2}}{m_{f_1'}+m_{f_2}}|\vec{q}|\vec{k}\right|\right)$$
$$\sqrt{\frac{\widehat{E}_{f_1'}\widehat{E}_{f1}}{4E_{f_1'}E_{f_1}}}\,\frac{p_z\left(p_x^2+p_y^2\right)|\vec{q}|}{\widehat{E}_{f_1'}\widehat{E}_{f1}}$$

$$V_{T\lambda=+1}^{(2^-)1}(|\vec{q}|) = i\frac{\sqrt{5}}{2}\sqrt{2m_I 2E_F(-\vec{q})}\int d^3p\,\frac{1}{4\pi|\vec{p}|^2}\left(\hat{\phi}^{(M_F(2^-))}_{f_1',f_2}(|\vec{p}|)\right)^*\hat{\phi}^{(M_I(0^-))}_{f_1,f_2}\left(\left|\vec{p}-\frac{m_{f_2}}{m_{f_1'}+m_{f_2}}|\vec{q}|\vec{k}\right|\right)$$
$$\sqrt{\frac{\widehat{E}_{f_1'}\widehat{E}_{f1}}{4E_{f_1'}E_{f_1}}}\left\{\left(p_z^2-p_x^2\right)\left(\frac{-p_z-\frac{m_{f_1'}}{m_{f_1'}+m_{f_2}}|\vec{q}|}{\widehat{E}_{f_1'}}-\frac{-p_z+\frac{m_{f_2}}{m_{f_1'}+m_{f_2}}|\vec{q}|}{\widehat{E}_{f_1}}\right)\right.$$
$$\left.-p_z p_y^2\left(\frac{1}{\widehat{E}_{f_1'}}-\frac{1}{\widehat{E}_{f_1}}\right)\right\}$$

$$V_{T\lambda=0}^{(2^-)3}(|\vec{q}|) = i\sqrt{\frac{15}{2}}\sqrt{2m_I 2E_F(-\vec{q})}\int d^3p\,\frac{1}{4\pi|\vec{p}|^2}\left(\hat{\phi}^{(M_F(2^-))}_{f_1',f_2}(|\vec{p}|)\right)^*\hat{\phi}^{(M_I(0^-))}_{f_1,f_2}\left(\left|\vec{p}-\frac{m_{f_2}}{m_{f_1'}+m_{f_2}}|\vec{q}|\vec{k}\right|\right)$$
$$\sqrt{\frac{\widehat{E}_{f_1'}\widehat{E}_{f1}}{4E_{f_1'}E_{f_1}}}\,p_z\left(p_x^2+p_y^2\right)\left(\frac{1}{\widehat{E}_{f_1'}}-\frac{1}{\widehat{E}_{f_1}}\right)$$

$$A^{(2^-)1}_{T\lambda=+1}(|\vec{q}|) = i\frac{\sqrt{5}}{2}\sqrt{2m_I 2E_F(-\vec{q})}\int d^3p\,\frac{1}{4\pi|\vec{p}|^2}\left(\hat{\phi}^{(M_F(2^-))}_{f_1',f_2}(|\vec{p}|)\right)^*\hat{\phi}^{(M_I(0^-))}_{f_1,f_2}\left(\left|\vec{p}-\frac{m_{f_2}}{m_{f_1'}+m_{f_2}}|\vec{q}|\vec{k}\right|\right)$$
$$\sqrt{\frac{\widehat{E}_{f_1'}\widehat{E}_{f1}}{4E_{f_1'}E_{f_1}}}\left\{\left(p_z^2-p_y^2\right)\left(1-\frac{(-\frac{m_{f_1'}}{m_{f_1'}+m_{f_2}}|\vec{q}|\vec{k}-\vec{p})\cdot(\frac{m_{f_2}}{m_{f_1'}+m_{f_2}}|\vec{q}|\vec{k}-\vec{p})}{\widehat{E}_{f_1'}\widehat{E}_{f1}}\right)\right.$$
$$\left.-p_z p_x^2|\vec{q}|\,\frac{m_{f_1'}-m_{f_2}}{m_{f_1'}+m_{f_2}}\,\frac{1}{\widehat{E}_{f_1'}\widehat{E}_{f_1}}\right\} \tag{A6}$$

- Case $J^\pi = 2^+$

$$V^{(D^*_{s2})1}_{T\lambda=+1}(|\vec{q}|) = i\frac{\sqrt{3}}{2}\sqrt{2m_I 2E_F(-\vec{q})}\int d^3p\,\frac{1}{4\pi|\vec{p}|}\left(\hat{\phi}^{(M_F(D^*_{s2}))}_{f_1',f_2}(|\vec{p}|)\right)^*\hat{\phi}^{(M_I(0^-))}_{f_1,f_2}\left(\left|\vec{p}-\frac{m_{f_2}}{m_{f_1'}+m_{f_2}}|\vec{q}|\vec{k}\right|\right)$$
$$\sqrt{\frac{\widehat{E}_{f_1'}\widehat{E}_{f1}}{4E_{f_1'}E_{f_1}}}\left(\frac{p_y^2-p_z^2-p_z|\vec{q}|\frac{m_{f_1'}}{m_{f_1'}+m_{f_2}}}{\widehat{E}_{f_1'}}-\frac{p_y^2-p_z^2+p_z|\vec{q}|\frac{m_{f_2}}{m_{f_1'}+m_{f_2}}}{\widehat{E}_{f_1}}\right)$$

$$A^{(D^*_{s2})0}_{T\lambda=0}(|\vec{q}|) = \frac{-i}{\sqrt{2}}\sqrt{2m_I 2E_F(-\vec{q})}\int d^3p\,\frac{1}{4\pi|\vec{p}|}\left(\hat{\phi}^{(M_F(D^*_{s2}))}_{f_1',f_2}(|\vec{p}|)\right)^*\hat{\phi}^{(M_I(0^-))}_{f_1,f_2}\left(\left|\vec{p}-\frac{m_{f_2}}{m_{f_1'}+m_{f_2}}|\vec{q}|\vec{k}\right|\right)$$
$$\sqrt{\frac{\widehat{E}_{f_1'}\widehat{E}_{f1}}{4E_{f_1'}E_{f_1}}}\left(\frac{p_x^2+p_y^2-2p_z^2-2p_z|\vec{q}|\frac{m_{f_1'}}{m_{f_1'}+m_{f_2}}}{\widehat{E}_{f_1'}}+\frac{p_x^2+p_y^2-2p_z^2+2p_z|\vec{q}|\frac{m_{f_2}}{m_{f_1'}+m_{f_2}}}{\widehat{E}_{f_1}}\right)$$

$$A^{(D^*_{s2})1}_{T\lambda=+1}(|\vec{q}|) = i\frac{\sqrt{3}}{2}\sqrt{2m_I 2E_F(-\vec{q})}\int d^3p\,\frac{1}{4\pi|\vec{p}|}\left(\hat{\phi}^{(M_F(D^*_{s2}))}_{f_1',f_2}(|\vec{p}|)\right)^*\hat{\phi}^{(M_I(0^-))}_{f_1,f_2}\left(\left|\vec{p}-\frac{m_{f_2}}{m_{f_1'}+m_{f_2}}|\vec{q}|\vec{k}\right|\right)$$
$$\sqrt{\frac{\widehat{E}_{f_1'}\widehat{E}_{f1}}{4E_{f_1'}E_{f_1}}}\left\{\,p_z\left(1-\frac{(-\frac{m_{f_1'}}{m_{f_1'}+m_{f_2}}|\vec{q}|\vec{k}-\vec{p})\cdot(\frac{m_{f_2}}{m_{f_1'}+m_{f_2}}|\vec{q}|\vec{k}-\vec{p})}{\widehat{E}_{f_1'}\widehat{E}_{f1}}\right)\right.$$
$$\left.+\frac{4p_z p_x^2-p_x^2|\vec{q}|\frac{m_{f_2}-m_{f_1'}}{m_{f_1'}+m_{f_2}}}{\widehat{E}_{f_1'}\widehat{E}_{f1}}\right\}$$

$$A^{(D^*_{s2})3}_{T\lambda=0}(|\vec{q}|) = -i\sqrt{2}\sqrt{2m_I 2E_F(-\vec{q})}\int d^3p\,\frac{1}{4\pi|\vec{p}|}\left(\hat{\phi}^{(M_F(D^*_{s2}))}_{f_1',f_2}(|\vec{p}|)\right)^*\hat{\phi}^{(M_I(0^-))}_{f_1,f_2}\left(\left|\vec{p}-\frac{m_{f_2}}{m_{f_1'}+m_{f_2}}|\vec{q}|\vec{k}\right|\right)$$
$$\sqrt{\frac{\widehat{E}_{f_1'}\widehat{E}_{f1}}{4E_{f_1'}E_{f_1}}}\left\{\,p_z\left(1-\frac{(-\frac{m_{f_1'}}{m_{f_1'}+m_{f_2}}|\vec{q}|\vec{k}-\vec{p})\cdot(\frac{m_{f_2}}{m_{f_1'}+m_{f_2}}|\vec{q}|\vec{k}-\vec{p})}{\widehat{E}_{f_1'}\widehat{E}_{f1}}\right)\right.$$
$$+\frac{1}{\widehat{E}_{f_1'}\widehat{E}_{f1}}\left[\,2p_z(-\frac{m_{f_1'}}{m_{f_1'}+m_{f_2}}|\vec{q}|-p_z)\cdot(\frac{m_{f_2}}{m_{f_1'}+m_{f_2}}|\vec{q}|-p_z)\right.$$
$$\left.\left.+\left(p_x^2+p_y^2\right)\left(-p_z+\frac{m_{f_2}-m_{f_1'}}{2(m_{f_1'}+m_{f_2})}|\vec{q}|\right)\right]\right\} \tag{A7}$$

[1] R. Aaij *et al*. (LHCb collaboration), Phys.Rev. **D87**, 112009 (2013), arXiv:1304.6317 [hep-ex].

[2] R. Aaij *et al*. (LHCb collaboration), Phys.Rev.Lett. (2013), arXiv:1304.6173 [hep-ex].
[3] D. Guadagnoli and G. Isidori, (2013), arXiv:1302.3909 [hep-ph].
[4] S. Blusk (LHCb Collaboration), (2012), arXiv:1212.4180 [hep-ex].
[5] R. Aaij *et al*. (LHCb collaboration), Phys.Rev. **D87**, 092007 (2013), arXiv:1302.5854 [hep-ex].
[6] R. Aaij *et al*. (The LHCb collaboration), (2013), arXiv:1308.4583 [hep-ex].
[7] R. Aaij *et al*. (LHCb collaboration), (2013), arXiv:1308.1428 [hep-ex].
[8] R. Aaij *et al*. (LHCb collaboration), Phys.Rev. **D87**, 071101 (2013), arXiv:1302.6446 [hep-ex].
[9] A. Dewhurst (ATLAS Collaboration), PoS **BEAUTY2011**, 013 (2011).
[10] G. Aad *et al*. (ATLAS Collaboration), JHEP **1212**, 072 (2012), arXiv:1208.0572 [hep-ex].
[11] G. Giurgiu, PoS **FPCP2010**, 014 (2010), arXiv:1010.4082 [hep-ex].
[12] A. Abulencia *et al.* (CDF Collaboration), Phys.Rev.Lett. **96**, 191801 (2006), arXiv:hep-ex/0508014 [hep-ex].
[13] L. Gong-Ru, L. Xin-Qiang, L. Yan-Min, and S. Fang, Acta Phys.Sin. **61**, 241301 (2012).
[14] Y. Amhis (LHCb Collaboration), PoS **HQL2012**, 034 (2012), arXiv:1207.4639 [hep-ex].
[15] D. van Eijk (LHCb collaboration), (2011), arXiv:1109.4276 [hep-ex].
[16] T. Kuhr (Belle Collaboration, CDF Collaboration, D0 Collaboration), Conf.Proc. **C100901**, 84 (2010), arXiv:1103.0896 [hep-ex].
[17] G. Giurgiu (CDF Collaboration), PoS **ICHEP2010**, 236 (2010), arXiv:1012.0962 [hep-ex].
[18] B. Batell and M. Pospelov, Phys.Rev. **D82**, 054033 (2010), arXiv:1006.2127 [hep-ph].
[19] A. Abulencia *et al.* (CDF Collaboration), Phys.Rev.Lett. **97**, 062003 (2006), arXiv:hep-ex/0606027 [hep-ex].
[20] N. Isgur and M. B. Wise, Phys.Lett. **B232**, 113 (1989).
[21] N. Isgur and M. B. Wise, Phys.Lett. **B237**, 527 (1990).
[22] H. Georgi, Phys.Lett. **B240**, 447 (1990).
[23] C. Albertus, E. Hernandez, J. Nieves, and J. Verde-Velasco, Phys.Rev. **D71**, 113006 (2005), arXiv:hep-ph/0502219 [hep-ph].
[24] E. Hernandez, J. Nieves, and J. Verde-Velasco, Eur.Phys.J. **A31**, 714 (2007), arXiv:hep-ph/0610125 [hep-ph].
[25] C. Albertus, E. Hernandez, J. Nieves, and J. Verde-Velasco, Eur.Phys.J. **A32**, 183 (2007), arXiv:hep-ph/0610030 [hep-ph].
[26] C. Albertus, E. Hernandez, and J. Nieves, Phys.Rev. **D85**, 094035 (2012), arXiv:1202.4861 [hep-ph].
[27] C. Albertus, E. Hernandez, and J. Nieves, Phys.Lett. **B704**, 499 (2011), arXiv:1108.1296 [hep-ph].
[28] R. Faustov and V. Galkin, Phys.Rev. **D87**, 034033 (2013), arXiv:1212.3167.
[29] R. Faustov and V. Galkin, Phys.Rev. **D87**, 094028 (2013), arXiv:1304.3255.
[30] J. Sun, Z. Xiong, Y. Yang, and G. Lu, Eur.Phys.J. **C73**, 2437 (2013), arXiv:1305.0691 [hep-ph].
[31] X. Yu, Z.-T. Zou, and C.-D. Lu, (2013), arXiv:1307.7485 [hep-ph].
[32] X. J. Chen, H. F. Fu, and G. L. Wang, J.Phys. G **39**, 045002.
[33] R.-H. Li, C.-D. Lu, and Y.-M. Wang, Phys.Rev. **D80**, 014005 (2009), arXiv:0905.3259 [hep-ph].
[34] K. Azizi, Nucl. Phys. B **801**, 70 (2008).
[35] K. Azizi and M. Bayar, Phys.Rev. **D78**, 054011 (2008), arXiv:0806.0578 [hep-ph].
[36] P. Blasi, P. Colangelo, G. Nardulli, and N. Paver, Phys.Rev. **D49**, 238 (1994), arXiv:hep-ph/9307290 [hep-ph].
[37] S.-M. Zhao, X. Liu, and S.-J. Li, Eur.Phys.J. **C51**, 601 (2007), arXiv:hep-ph/0612008 [hep-ph].
[38] M. A. Ivanov, J. G. Korner, and P. Santorelli, Phys.Rev. **D71**, 094006 (2005), arXiv:hep-ph/0501051 [hep-ph].
[39] J. Beringer *et al.* (Particle Data Group), Phys. Rev. D **86**, 010001 (2012).
[40] E. Hernandez, J. Nieves, and J. Verde-Velasco, Phys.Rev. **D74**, 074008 (2006), arXiv:hep-ph/0607150 [hep-ph].
[41] R. Bhaduri, L. Cohler, and Y. Nogami, Nuovo Cim. **A65**, 376 (1981).
[42] B. Silvestre-Brac, Few Body Syst. **20**, 1 (1996).
[43] J. Korner and G. Schuler, Z.Phys. **C46**, 93 (1990).
[44] J. Segovia, C. Albertus, D. Entem, F. Fernandez, E. Hernandez, *et al.*, Phys.Rev. **D84**, 094029 (2011), arXiv:1107.4248 [hep-ph].
[45] J. Vijande, F. Fernandez, and A. Valcarce, J.Phys. **G31**, 481 (2005), arXiv:hep-ph/0411299 [hep-ph].
[46] D. Ebert, R. Faustov, and V. Galkin, Phys.Rev. **D75**, 074008 (2007), arXiv:hep-ph/0611307 [hep-ph].
[47] M. Beneke, G. Buchalla, M. Neubert, and C. T. Sachrajda, Phys.Rev.Lett. **83**, 1914 (1999), arXiv:hep-ph/9905312 [hep-ph].
[48] M. A. Ivanov, J. G. Korner, and P. Santorelli, Phys.Rev. **D73**, 054024 (2006), arXiv:hep-ph/0602050 [hep-ph].
[49] K. Azizi, R. Khosravi, and F. Falahati, Int.J.Mod.Phys. **A24**, 5845 (2009), arXiv:0811.2671 [hep-ph].
[50] R.-H. Li, C.-D. Lu, and H. Zou, Phys.Rev. **D78**, 014018 (2008), arXiv:0803.1073 [hep-ph].
[51] M. A. Ivanov, J. G. Korner, S. G. Kovalenko, P. Santorelli, and G. G. Saidullaeva, Phys.Rev. **D85**, 034004 (2012), arXiv:1112.3536 [hep-ph].